Leids Universitair Medisch Centrum

Association between the macrocirculation and the mitochondrial oxygenation in critically ill patients with sepsis

Fleur Brouwer

TECHNICAL MEDICINE
MASTER THESIS

Association between the macrocirculation and the mitochondrial oxygenation in critically ill patients with sepsis

by

F. Brouwer
4299515

Final version | 25 June 2020

Thesis in partial fulfilment of the requirements for the joint degree of Master of Science in
Technical Medicine
University Leiden ; Delft University of Technology ; Erasmus University Rotterdam

Master thesis project (TM30004 ; 35 ECTS)
Dept. of Biomechanical Engineering, TU Delft
November 2019 – June 2020

Supervisor(s):

Medical supervisor	Dr. M.S. Arbous
Technical supervisor	Dr. ir. A.C. Schouten

Thesis committee members:

Core members

Prof. dr. ir. J. Harlaar	TU Delft, chair
Dr. M.S. Arbous	LUMC, medical supervisor
Dr. ir. A.C. Schouten	TU Delft, technical supervisor

Extra members

Prof. Ir. P.J. French	TU Delft, dept bioelectronics
Dr. D. DoDou	TU Delft, examination Board Technical Medicine

Universiteit Leiden

TU Delft Delft University of Technology

Erasmus University Rotterdam

Abstract

Introduction

The Cellular Oxygen METabolism (COMET) monitor measures mitochondrial oxygen tension ($mitoPO_2$) in vivo at the bedside with delayed fluorescence of mitochondrial protoporphyrin (PpIX). Blocking microcirculatory oxygen supply by pressing the measurement probe on the skin allows the measurement of mitochondrial oxygen consumption ($mitoVO_2$). Combining the static mitochondrial parameter (i.e. $mitoPO_2$) and the dynamic mitochondrial parameter (i.e. $mitoVO_2$) can provide useful information about different aspects of the mitochondrial function in sepsis. However, it is not yet known how these mitochondrial parameters relate to the traditional systemic hemodynamic parameters, such as lactate and central venous oxygen saturation ($ScvO_2$). The first aim of this study is to develop an analysis method to derive a measure for oxygen consumption. The second aim of this study is to investigate the association between the macrocirculation and the mitochondrial oxygenation, in particular $mitoPO_2$ and $mitoVO_2$, and to investigate the association between these two mitochondrial parameters in critically ill patients with sepsis.

Methods

We performed a prospective observational study in critically ill patients with suspicion of sepsis who were admitted to the Intensive Care Unit of the Leiden Medical University Center. A patch containing 5-aminolevulinic (ALA) was placed on the anterior chest wall of the patient to induce PpIX in the mitochondria. $MitoPO_2$ was measured by the oxygen-dependent fluorescence of mitochondrial PpIX. $MitoVO_2$ was determined by a dynamic $mitoPO_2$ measurement (taking up a series of $mitoPO_2$ samples) while blocking the microcirculatory oxygen supply by applying pressure with the measurement probe of the COMET monitor. $MitoPO_2$ samples and blood samples were collected at the same predefined time points. A sigmoid function was used to fit the raw $mitoPO_2$ signal of the dynamic $mitoPO_2$ measurements. A mixed linear model was used to study the association between the macrocirculation and the mitochondrial oxygenation and the association between the mitochondrial oxygenation and oxygen consumption. For this second model, we divided the $mitoPO_2$ levels into a low, medium and high $mitoPO_2$ group.

Results

A total of 202 $mitoPO_2$ measurements were performed in 41 critically ill patients with sepsis. However, due to poor signal quality or insufficient fit performance, 29 (14%) dynamic $mitoPO_2$ measurements of different patients were excluded for further analysis. The results of this study showed that higher $mitoPO_2$ levels were significantly associated with lower lactate levels (β = -0.002744, p = 0.023). Moreover, $mitoPO_2$ levels of the low $mitoPO_2$ group were significantly associated with higher $mitoVO_2$ rates (β = 0.103822, $p < 0.001$). Interestingly, $mitoVO_2$ could not be induced in 31 (15%) dynamic $mitoPO_2$ measurements.

Conclusion

These results show that $mitoPO_2$ levels are associated with lactate levels in critically ill patients with sepsis. Mitochondria with low oxygen levels are in stress and will switch to anaerobic metabolism leading to lactate production. Moreover, these mitochondria have no reserves and will directly suffer from the acute cessation of the oxygen supply because these mitochondria consume the present oxygen faster compared to the mitochondria with higher $mitoPO_2$ levels.

Keywords: sepsis, mitochondria, mitochondrial oxygen tension, mitochondrial oxygen consumption, COMET

Introduction

Resuscitating critically ill septic patients remains a challenge in intensive care medicine. Safeguarding an adequate oxygen transport to organs and tissues by administration of fluids, blood transfusion, vasoactive and inotropic medication is the primary goal of current resuscitation procedures. These procedures are aimed at the correction of systemic hemodynamic parameters, such as blood pressure, cardiac output, lactate and central venous oxygen saturation ($ScvO_2$). It is expected that normalization of the macrocirculation will result in a parallel improvement of the microcirculatory perfusion and optimized oxygen supply to parenchymal cells to establish aerobic metabolism (1). The condition in which this parallel improvement is in place is called hemodynamic coherence (1).

However, loss of hemodynamic coherence is frequently present in septic patients in whom the microcirculation fails to transport oxygen to the parenchymal cells despite successful macrocirculatory resuscitation (2-6). The microcirculation can be assessed by bedside tools that allow direct visualization of the microcirculation under the patient's tongue (7-8). Pathological heterogeneity of microcirculatory perfusion leading to functional shunting can cause a reduced capacity of the tissues to extract oxygen and thus cellular hypoxia (1,6). However, these microcirculatory alterations are not the only cause of this defect in oxygen extraction since normalization of both the macro- and microcirculation does not always lead to clinical improvement (9-11). This suggests that other mechanisms, such as mitochondrial dysfunction, also might play a role in the pathogenesis of cellular and tissue hypoxia in sepsis (12-14). However, the literature about the role of mitochondrial dysfunction in sepsis is controversial (15). Information about the mitochondrial function is useful for monitoring the effectiveness of therapies in optimizing oxygen transport to organs and tissues.

To further unravel the mitochondrial dysfunction in sepsis and to better understand the complex relationship between the macrocirculation, microcirculation and cellular oxygenation in sepsis, we need a tool that allows us to look beyond the microcirculation into the parenchymal cells, monitoring aspects of mitochondrial function. However, the possibilities for monitoring mitochondrial function in critically ill patients with sepsis are limited since only ex vivo techniques are available. Measurements in suspensions of isolated cells or isolated mitochondria might not adequately reflect the in vivo situation of the mitochondrial function in a critically ill septic patient (16).

The protoporphyrin IX-triplet state lifetime technique (PpIX-TSLT) provides new opportunities to monitor the mitochondrial function in vivo non-invasively (17). This technique enables measurements of the mitochondrial oxygen tension ($mitoPO_2$) by means of the delayed fluorescence of PpIX, the final precursor of the heme biosynthesis pathway in mitochondria. PpIX-TSLT is the first technique that can measure $mitoPO_2$ in living cells and in vivo in animals (17-20). Further development of this technique currently allows $mitoPO_2$ measurement in the human skin at the bedside (20-22). In addition to $mitoPO_2$, it is also technically possible to gain information about mitochondrial oxygen consumption ($mitoVO_2$), which can be determined by dynamic $mitoPO_2$ measurements while blocking the local microcirculatory blood flow (23). This mitochondrial parameter, besides $mitoPO_2$,may provide new insight into mitochondrial oxygen metabolism.

The application of the PpIX-TLST in the clinical setting has been enabled by the development of the Cellular Oxygen METabolism (COMET) monitor (24). So far, the feasibility of the COMET monitor has successfully been tested in healthy volunteers (25-26) and critically ill patients with sepsis (27). The COMET monitor is able to provide insight into the oxygen balance, i.e. the balance between oxygen supply and oxygen consumption, at the mitochondrial level. Hence, the COMET monitor provides important information about different aspects of the mitochondrial function in sepsis. However, it is not yet known how the mitochondrial parameters ($mitoPO_2$ and $mitoVO_2$) relate to the traditional systemic hemodynamic parameters. The first aim of this study is to develop an analysis method to derive a measure for oxygen consumption from dynamic $mitoPO_2$ measurements. The second aim of this study is to investigate the association between the macrocirculation and the mitochondrial oxygenation, in particular $mitoPO_2$ and $mitoVO_2$, and to investigate the association between these two mitochondrial parameters in critically ill patients with sepsis.

Methods

Principle of mitoPO₂ measurements

The principle of the PpIX-TSLT has been described in detail elsewhere (17-18, 28). In short, PpIX-TSLT uses the oxygen-dependent optical properties of the PpIX protein to measure mitoPO$_2$. PpIX is synthesized in the mitochondria as the final precursor of heme (29). Topical administration of 5-aminolevulinic acid (ALA), the precursor of PpIX, by a specific ALA patch enhances the PpIX concentration inside the mitochondria because the incorporation of iron in the PpIX molecule is a rate-limiting step in the heme biosynthetic pathway (**Figure 1**).

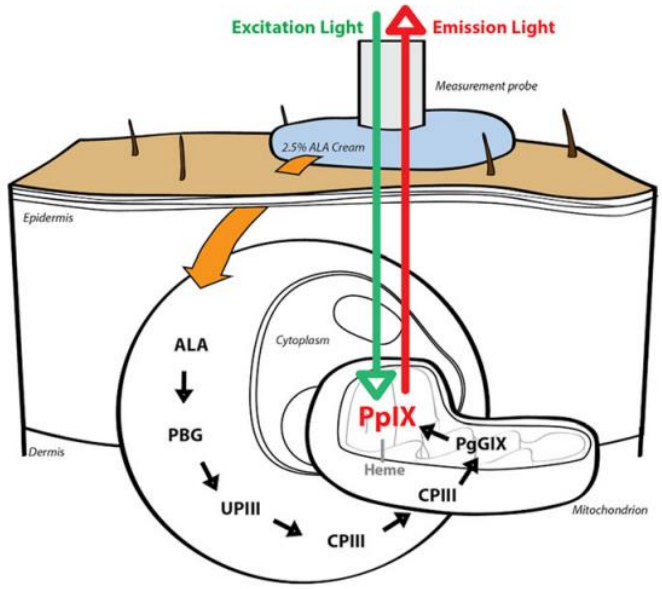

Figure 1: The pathway by which topical ALA administration enhances mitochondrial PpIX because the conversion of PpIX to heme is a rate-limiting step.
ALA 5-aminolevulinic acid, CPIII coproporphyrinogen III, PBG porphobilinogen, PO2 oxygen tension, PpIX protoporphyrin IX, UPIII uroporphyrinogen III
Reprinted from: Harms et.al. (45).

When PpIX is excited by an excitation pulse with green light, PpIX turns into its excited triplet state (T_1). PpIX can directly relax to its ground state (S_0) by spontaneous relaxation through emission of red delayed fluorescence (**Figure 2**). However, relaxation to S_0 can also occur by collision with a triplet state molecule such as oxygen. During a collision, the oxygen molecule absorbs the energy from PpIX resulting in relaxation of PpIX without light emission (**Figure 2**). This process is called "triplet-state quenching".

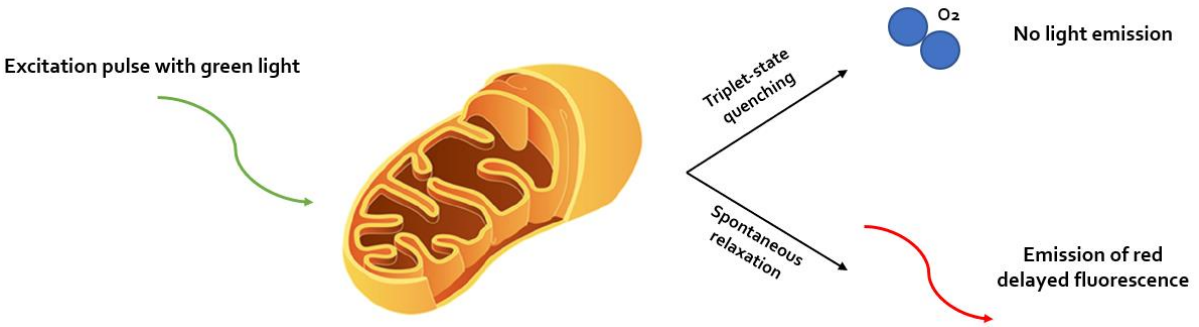

Figure 2: Principle of the protoporphyrin IX(PpIX)-triplet state lifetime technique. After an excitation pulse with green light, PpIX possesses an excited triplet and causes the emission of red delayed fluorescence. However, the excited triplet state reacts strongly with oxygen. Collision with an oxygen molecule is called triplet-state quenching. Triplet-state quenching results in the relaxation of PpIX without light emission.

Quenching of the triplet state is a process that makes the PpIX-TLST dependent on the collision frequency. The collision frequency is determined by the chance that a single oxygen molecule causes a quenching event (*kq*) and the oxygen concentration in the mitochondria. Triplet-state quenching results in the relaxation of PpIX without light emission and therefore will shorten the delayed fluorescence lifetime (**Figure 3**).

The delayed fluorescence lifetime is related to mitoPO$_2$ according to the Stern-Volmer equation:

$$mitoPO2 = \frac{\frac{1}{\tau} - \frac{1}{\tau 0}}{kq}$$

in which τ is the measured delayed fluorescence lifetime, τo is the measured delayed fluorescence lifetime in the absence of oxygen and *kq* is the quenching constant (the chance that a single oxygen molecule causes a quenching event).

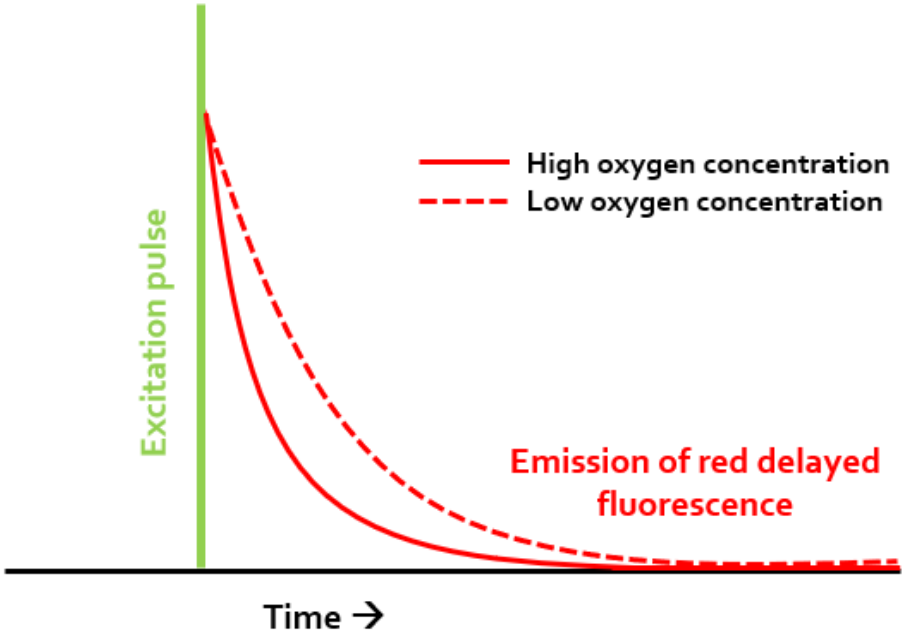

Figure 3: Protoporphyrin IX (PpIX) emits red delayed fluorescence after excitation by a pulse of green light. The delayed fluorescence lifetime depends on the oxygen concentration in the mitochondria. High oxygen concentration will increase the collision frequency. Collisions of PpIX with oxygen will shorten the delayed fluorescence lifetime.

The COMET monitor enables physicians to measure mitoPO$_2$ at the bedside using the PpIX-TLST (24). This monitor uses a measurement probe with a green light pulse laser to excite the accumulated PpIX in the mitochondria. The red delayed fluorescent signal is detected by a photomultiplier tube. For analysis of each red delayed fluorescence signal, the COMET monitor uses the Stern-Volmer equation to automatically calculate the mitoPO$_2$ in the measurement volume under the probe. The COMET monitor also automatically calculates the corresponding signal-to-noise ratio (SNR) value for each mitoPO$_2$ sample. A higher SNR corresponds to a stronger red delayed fluorescence signal and a more sensitive mitoPO$_2$ measurement. SNR is calculated and defined as the ratio of maximum amplitude of the red delayed fluorescence signal to the maximum amplitude of the noise signal (18). The COMET monitor operates reliably at SNR ≥ 5 (24). Therefore, we chose to define an SNR of 5 as the minimum required signal quality for a feasible mitoPO$_2$ measurement.

Principle of mitoVO$_2$ measurements

MitoVO$_2$ is measured by means of the mitochondrial oxygen disappearance rate (ODR) after local occlusion of the microcirculation (**Figure 4**) (23). This local occlusion was obtained by application of pressure with the measurement probe of the COMET monitor on the skin. This procedure created the possibility to measure the decrease in mitoPO$_2$ over time, due to blockade of the microcirculatory oxygen supply and ongoing cellular/mitochondrial oxygen consumption. MitoVO$_2$ can be calculated from the descending part (e.g. the mitochondrial oxygen consumption phase) of the raw mitoPO$_2$ signal (**Figure 4**).

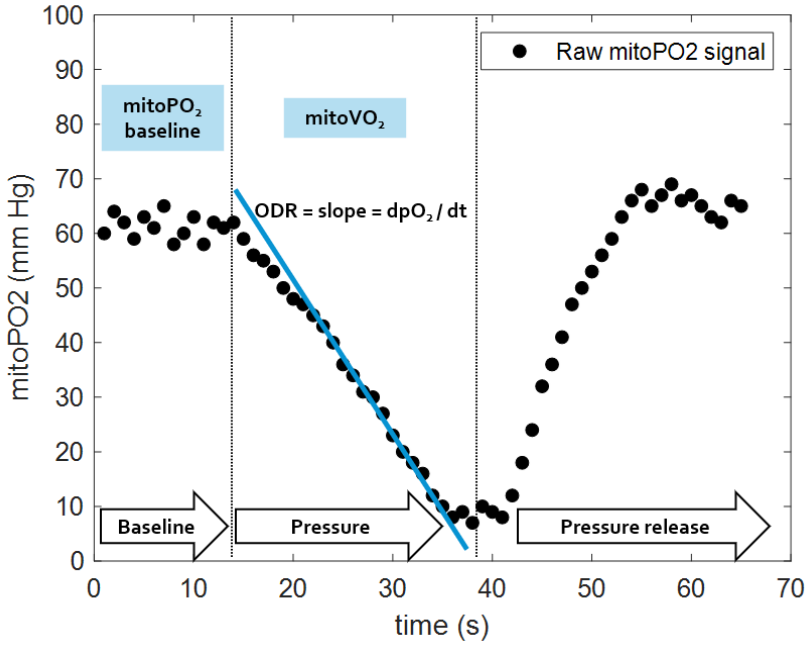

Figure 4: Description of a dynamic mitoPO$_2$ measurement to obtain the baseline mitochondrial oxygen tension (mitoPO$_{2_baseline}$) and mitochondrial oxygen consumption (mitoVO$_2$). A dynamic mitoPO$_2$ measurement is a series of up to 120 mitoPO$_2$ samples acquired at 1 Hz. In the first 10 seconds, a mitoPO$_2$ baseline was measured. Subsequently, pressure was applied on the measurement probe for approximately 30-45 seconds to stop the microcirculatory blood flow in the measurement volume under the probe to evaluate the mitoVO$_2$. Finally, the pressure was released to restore the microcirculatory blood flow and mitochondrial reoxygenation.

Study population

The study population consisted of critically ill patients with (the suspicion of) sepsis who were admitted via the emergency department (ED) or hospital ward to the Intensive Care Unit (ICU) of Leiden University Medical Centre (LUMC). Sepsis was defined as 'a life-threatening organ dysfunction caused by a dysregulated host response to an infection' (16). Septic patients were identified as specified in the protocol of sepsis identification and management in the emergency department, consisting of having clinical suspicion of sepsis in combination with at least two the following symptoms: (1) ≥ 20 breaths per minute, (2) heart frequency > 90 beats per minute, (3) leukocytes > 12*10^9 or leukocytes < 4*10^9, and/or (4) temperature > 38 °C or < 36 °C (30). Patients were required to be at least 18 years old, to provide direct or deferred informed consent and to have an arterial catheter in situ, since arterial blood samples were taken regularly for the study. Informed consent was sought in the ED or the hospital ward when it was known that a patient with sepsis was going to be admitted to the ICU. If the patient was too ill to comprehend the informed consent, it was sought from his or her legal representative. However, if the patient or legal representative could not have been reached in time for written informed consent, while the patient met the eligibility criteria, the patient was included with a deferred consent procedure. Informed consent was sought within 48 hours after the inclusion of the patient.

Patients with sepsis discharged after ED visit or admitted to a hospital ward other than the ICU after ED visit were excluded from the study. Other exclusion criteria were: porphyria and/or photo dermatosis since the risk of phototoxicity, hypersensitivity to the contents of the ALA patch, pregnant or breastfeeding women since there is no data from the use of the ALA patch in this population and insufficient comprehensibility of the Dutch language.

Experimental set-up

Experimental preparation

Reliable measurements can only take place with suitable PpIX concentrations inside the mitochondria. Therefore, at least four hours before the first measurement, a self-adhesive patch containing ALA was placed on the anterior chest wall (next to the sternum) for the induction of PpIX. Present hair was shaved and the skin was rubbed with alcohol to remove the first layers of the stratum corneum to enhance ALA penetration. After ALA patch placement, the outline of the ALA patch was marked and a skin pad was placed over the ALA patch to protect the skin from ambient light to create reliable measurements.

While waiting for the induction of PpIX after placement of the ALA patch, demographic and clinical information about the patient was gathered. Gender, age, sepsis source and Acute Physiology and Chronic Health Evaluation (APACHE) IV score were obtained from the hospital's electronic patient dossier system. Four hours after PpIX induction, the ALA patch was temporarily removed and mitoPO$_2$ was measured by placing the measurement probe of the COMET monitor on the marked part on the skin where PpIX was induced.

The COMET monitor provides two different measurement types, namely a single mitoPO$_2$ measurement and a dynamic mitoPO$_2$ measurement. During a single mitoPO$_2$ measurement, the measurement probe of the COMET monitor makes light contact with the skin and one mitoPO$_2$ sample is measured for each excited green light pulse. No pressure is applied during a single mitoPO$_2$ measurement. The COMET monitor can also provide mitoPO$_2$ measurements in a dynamic situation by taking a series of up to 120 mitoPO$_2$ samples acquired at 1 Hz. During this dynamic mitoPO$_2$ measurement pressure can be applied on the measurement probe to determine mitoVO$_2$.

When starting the COMET monitor, the laser must be warmed up so that the laser has sufficient excitation power. After placing the measurement probe on the skin, calibration measurements were performed to ensure the quality of the subsequent dynamic mitoPO$_2$ measurements. Thereafter, five single mitoPO$_2$ measurements were performed in the first minute to establish a reliable and stable mitoPO$_2$ measurement. These calibration measurements were followed by the first dynamic mitoPO$_2$ measurement (**Figure 4**). During this dynamic mitoPO$_2$ measurement, a baseline mitoPO$_2$ was measured for 10 seconds in an undisturbed situation. Subsequently, pressure was applied on the measurement probe for about 30-45 seconds to stop microcirculatory blood flow in the marked part of the skin. After this period, the pressure was released to restore the microcirculatory blood flow and mitochondrial reoxygenation. Room lights were turned off during all the measurements to minimize the effect on ambient light. Directly after the dynamic mitoPO$_2$ measurement, the ALA patch was replaced on the marked part of the skin to protect the skin against phototoxicity and to keep mitochondrial PpIX at suitable concentrations.

Dynamic mitoPO$_2$ measurements were performed at predefined time points. After the first dynamic mitoPO$_2$ measurement (= T0), dynamic mitoPO$_2$ measurements were repeated every two hours (= T1a-z) until 6 PM (= T2). Between 6 PM and 12 AM, dynamic mitoPO$_2$ measurements were performed at 8 PM (= T3), 10 PM (= T4) and midnight (= T5). The last dynamic mitoPO$_2$ measurement was performed 24 hours after the first dynamic mitoPO$_2$ measurement (= T6). The COMET monitor was not turned off between the measuring moments on the same day and therefore the calibration measurements do not have to be performed before each dynamic mitoPO$_2$ measurement, only before the first dynamic mitoPO$_2$ measurement of that day.

The dynamic mitoPO$_2$ measurements of each predefined time point were stored in separate datasets. The SNR for each mitoPO$_2$ sample was also documented in these datasets. An overview of the mitoPO$_2$ measurements during the study is given in **Figure 5**.

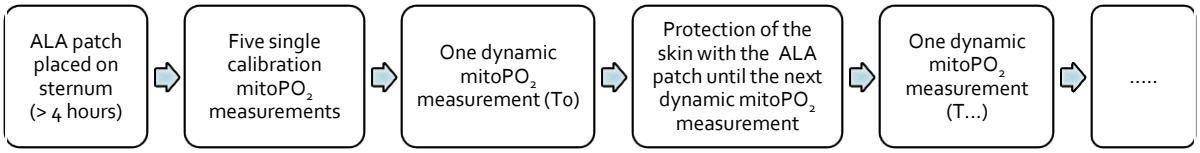

Figure 5: An overview of the mitochondrial oxygen tension ($mitoPO_2$) measurements during the study. A 5-aminolevulinic acid (ALA) patch was placed on the chest wall for induction of Protoporphyrin IX (PpIX), for at least four hours before the first measurement can take place. After placing the measurement probe for the first time that day, five single calibration $mitoPO_2$ measurements were made to ensure the quality of the subsequent dynamic $mitoPO_2$ measurements. After these calibration measurements, a series of $mitoPO_2$ samples was measured during a dynamic $mitoPO_2$ measurement. During this dynamic $mitoPO_2$ measurement, pressure was applied on the measurement probe to stop microcirculatory blood flow. After the dynamic $mitoPO_2$ measurement, the ALA patch was replaced on the marked part of the skin.

In addition to the $mitoPO_2$ measurements, blood samples were taken at the same predefined timepoints. Lactate and $ScvO_2$ (if applicable) were collected through an arterial catheter and a central venous catheter. In the LUMC, it is standard clinical practice that patients receive an arterial catheter when they are admitted to the ICU. In contrast, a central venous catheter is only placed when indicated. If a central venous catheter was not present in the patient, no $ScvO_2$ samples were collected.

Data analysis

A self-developed MATLAB (MATLAB and Statistics Toolbox 2019a, The MathWorks) script was used for data preparation and calculation of the mitochondrial parameters (**APPENDIX I**). This MATLAB script is the final result of an interim analysis focusing on different analysis methods to derive a measure for $mitoVO_2$ from a dynamic $mitoPO_2$ measurement (**APPENDIX II**). This MATLAB script calculates the baseline mitochondrial oxygen tension ($mitoPO_{2\_baseline}$) and the maximum oxygen consumption ($mitoVO_{2\_max}$) of a dynamic $mitoPO_2$ measurement (**Figure 4**).

Data preparation

Since the COMET monitor operates reliably at SNR ≥ 5, only $mitoPO_2$ samples with an SNR ≥ 5 were analyzed. Therefore, one, two or three consecutive $mitoPO_2$ samples of a dynamic $mitoPO_2$ measurement with an SNR < 5 were interpolated. If more than three consecutive $mitoPO_2$ samples of a dynamic $mitoPO_2$ measurement had an SNR < 5, the dynamic $mitoPO_2$ measurement was considered as unreliable and was removed from the database.

Calculation of the mitochondrial parameters

After data preparation, the raw $mitoPO_2$ signal of each dynamic $mitoPO_2$ measurement was smoothed by a Gaussian filter. This Gaussian smoothed $mitoPO_2$ signal and its first derivative were used to estimate the initial parameters of two complementary sigmoid functions.

These two functions were used to fit the raw $mitoPO_2$ signal of each dynamic $mitoPO_2$ measurement (25):

$$\frac{K1}{1+e^{(-B1*(x-M1))}}+\frac{K2}{1+e^{(-B2*(x-M2))}}+Z$$

K1 = baseline $mitoPO_2$ level before inhibition of the microcirculation
K2 = $mitoPO_2$ level after reoxygenation
B1 = slope modulation for oxygen consumption
B2 = slope modulation for reoxygenation
M1 = time of maximum oxygen consumption during inhibition of the microcirculation
M2 = time of maximum reoxygenation after pressure release
Z = minimum $mitoPO_2$ level after inhibition of the microcirculation

If the dynamic mitoPO$_2$ measurement did not contain an ascending part, only a single sigmoid function was used to fit the descending part of the raw mitoPO$_2$ signal:

$$\frac{K1}{1 + e^{(-B1*(x-M1))}} + Z$$

K1 = baseline mitoPO$_2$ level before inhibition of the microcirculation
B1 = slope modulation for oxygen consumption
M1 = time of maximum oxygen consumption during inhibition of the microcirculation
Z = minimum mitoPO$_2$ level after inhibition of the microcirculation

After fitting, the fitted curve was optimized by re-estimating the initial parameters of the two complementary sigmoid functions. These parameters were re-estimated based on the first derivative of the fitted curve. In this way, a second optimized fitted curve was created. If this optimized fitted curve did not adequately detect the baseline of the dynamic mitoPO$_2$ measurement, the first part of the optimized fitted curve was manually replaced by the first part of the Gaussian smoothed mitoPO$_2$ curve.

MitoPO$_{2_baseline}$ was determined by averaging the first three mitoPO$_2$ samples of the dynamic mitoPO$_2$ measurement (**Figure 6**). However, if the variance between these three mitopO$_2$ samples was greater than 20, it was assumed that the mitoPO$_2$ directly descends at the beginning of the dynamic mitoPO$_2$ measurement. In that case, the first mitoPO$_2$ sample was selected as mitoPO$_{2_baseline}$. MitoVO2$_{_max}$ was determined via the minimum value of the first derivative of the optimized fitted curve (**Figure 6**).

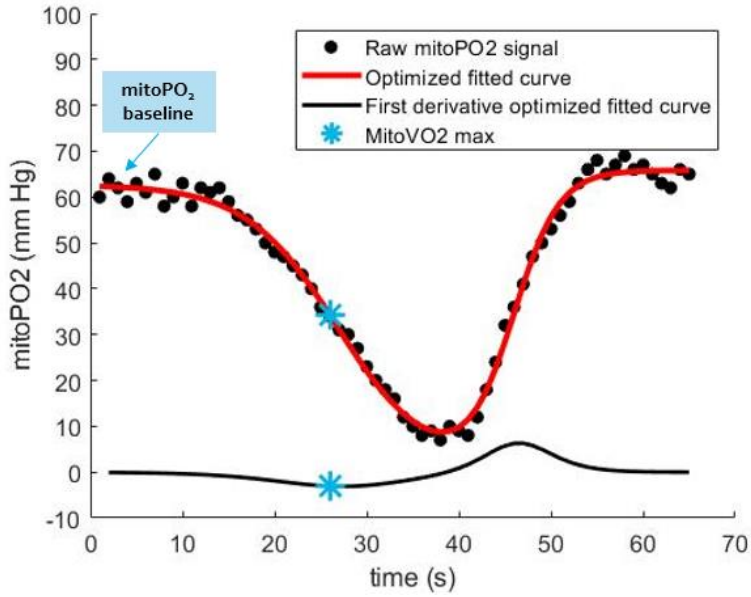

Figure 6: Illustration of the raw mitochondrial oxygen tension (mitoPO$_2$) signal and the optimized fitted curve to calculate maximum oxygen consumption (mitoVO$_{2_max}$) using the maximum slope of the optimized fitted curve.

For each dynamic mitoPO$_2$ measurement, the performance of the descending part of the optimized fitted curve was derived by the root mean square error (RMSE) function. The starting point and endpoint of the descending part of the optimized fitted curve were determined by the curvature formula (**Figure 7A**) (31). This formula indicates how fast the optimized fitted curve changes direction at each time point (**Figure 7B**).

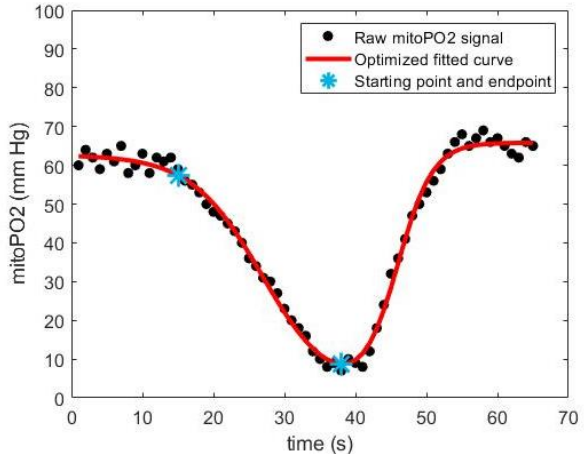

Figure 7A

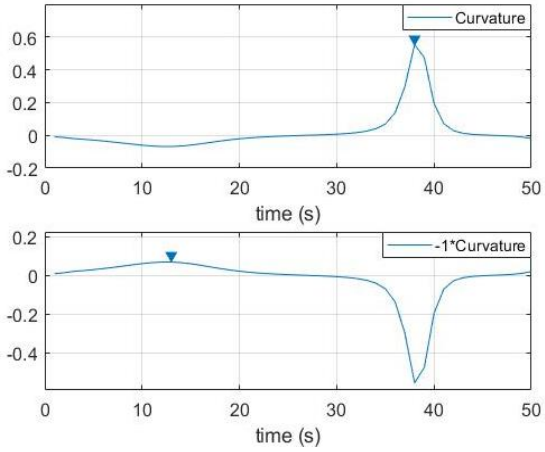

Figure 7B

Figure 7A: The starting point and endpoint of the descending of the optimized fitted curve. These points were determined by the curvature formula.
Figure 7B: The curvature indicates how fast the optimized fitted curve changes direction at each time point. If the curvature is positive then the graph has an upward concavity and if the curvature is negative the graph has a downward concavity.

The RMSE function was defined as the sum of the square of the error between raw mitoPO$_2$ signal (data) and the optimized fitted curve (fit) between the starting point and endpoint of the descending part of the optimized fitted curve:

$$RMSE = \frac{\sqrt{\sum_{tstart}^{tend}(fit - data)^2}}{N}$$

where *N* is the number of mitoPO$_2$ samples between, *tstart* is the starting point and *tend* is the endpoint of the descending part of the optimized fitted curve.

If the RMSE of the descending part of the optimized fitted curve was greater than five, the performance of the optimized fitted curve was visually assessed. If the fit performance was insufficient, the dynamic mitoPO$_2$ measurement was removed from the database. A more comprehensive overview of the MATLAB script can be found in **APPENDIX I**.

Statistical analysis

Statistical analysis was performed with SPSS Statistics Version 25. Descriptive statics was used to describe the characteristics of the study population. Parametric distributed continuous variables were presented as mean with standard deviation, and non-parametric continuous variables were presented as median with interquartile range. The parametric distribution of the variables was assessed with histograms and normal quartile plots. Categorical variables were stated as numbers and percentages.

The database was transformed into a longitudinal database to describe the change of mitoPO$_{2_baseline}$, mitoVO$_{2_max}$, lactate and ScvO$_2$ over time with graphs. Time was set as a continuous variable and defined as the number of hours between the dynamic mitoPO$_2$ measurements at time point 'x' and the first dynamic mitoPO$_2$ measurement of each patient.

This longitudinal database requires a special statistical method since the set of measurements within one patient were correlated. Therefore a mixed linear model was used to analyze our longitudinal database. When several different models were fitted on the database, the best fitting model was selected by the smallest Akaike information error (AIC) (32). The mixed linear model with random intercept per individual patient and first-order autoregressive of order 1 (AR1) as covariance type had the smallest AIC error. The AR1 structure considers that for each patient the association between two parameters depends on the distance in time between two measurements. The linear mixed model was adjusted for confounders: age, gender, sepsis source and APACHE score. Covariates (continuous variables), factors (categorical variables) and time were set as fixed effects in our mixed linear model.

First, a model was constructed with lactate or $ScvO_2$ as dependent variable and $mitoPO_{2\_baseline}$ or $mitoVO_{2\_max}$ as covariate to assess the association between the macrocirculation and mitochondrial oxygenation in critically ill patients with sepsis. A second model was constructed with $mitoVO_{2\_max}$ as dependent variable and $mitoPO_{2\_baseline}$ as covariate to assess the association between the static mitochondrial parameter, i.e. mitochondrial oxygenation at baseline, and the dynamic mitochondrial parameter, i.e. oxygen consumption during the blockade of microcirculatory oxygen supply (**APPENDIX III**). For this model, $mitoPO_{2\_baseline}$ was divided into three equal groups: low $mitoPO_{2\_baseline}$) 0-40 mm Hg, medium $mitoPO_{2\_baseline}$) 41-62.3 mm Hg, high low $mitoPO_{2\_baseline}$) > 62.3 mm Hg. Visual binning was used to identify suitable cut-off points to divide $mitoPO_{2\_baseline}$ into these three equal groups. For all analyses, a p-value of 0.05 was considered as statistically significant.

Results

Of the 100 screened patients, 42 septic patients were included in the analysis after assessment of eligibility. However, after the first dynamic mitoPO$_2$ measurement, one patient was excluded due to an allergic reaction to the ALA patch, yielding a total of 41 patients with sepsis. The patient characteristics are summarized in **Table 1**. Patient's ages ranged from 34 to 82 years (mean = 64.0, standard deviation = 11.4) and most patients were male (n = 30, 73.2%). The most common source of sepsis was pulmonary (n = 14, 34.1%). The mean APACHE IV score was 73.6 ± 25.5.

Table 1: Characteristics of the patient population

Characteristics	Overall, n = 41
Age in years, mean ± SD	64.0 ± 11.4
Male, absolute number (%)	30 (73.2%)
Sepsis sources, absolute number (%)	
Unknown	2 (4.9%)
Cutaneous	3 (7.3%)
Gastrointestinal	12 (29.3%)
Urinary	7 (17.1%)
Pulmonary	14 (34.1%)
Other	3 (7.3%)
APACHE score, mean ± SD	73.6 ± 25.5

APACHE IV score = Acute Physiologic and Chronic Health Evaluation IV score; SD = standard deviation

Primary analysis

A total of 202 PpIX-TLST measurements were performed on the 41 included septic patients. Due to poor signal quality at the beginning of dynamic mitoPO$_2$ measurement, it was not possible to calculate the mitoPO$_{2_baseline}$ in 7 dynamic mitoPO$_2$ measurements from 5 patients. In addition, due to poor signal quality later in the dynamic mitoPO$_2$ measurement, 22 dynamic mitoPO$_2$ measurements of 13 patients were excluded for further analysis. Moreover, due to an insufficient fit performance, 7 dynamic mitoPO$_2$ measurements of 7 patients were excluded for further analysis. ScvO$_2$ samples were collected from 15 patients. A total overview of all the dynamic mitoPO$_2$ measurements of each patient at each time point can be found in **APPENDIX IV**. The descriptive statistics are summarized in **Table 2**.

Table 2: Descriptive statistics for the aggregated time points

Aggregated time points	Parameter	[Unit]	n	Mean ± SD	Median (IQR)
0-3hr	$mitoPO_{2\_baseline}$	mm Hg	79	52.7 ± 27.7	52.0 (39.7-63.0)
	$mitoVO_{2\_max}$	[mm Hg/s]	64	2.7 ± 2.7	2.3 (0.1-3.9)
	Lactate	mmol / L	72	2.4 ± 2.0	1.8 (1.2-2.8)
	$ScvO_2$	%	21	77.1 ± 11.2	80 (73.0-84.0)
4-7hr	$mitoPO_{2\_baseline}$	mm Hg	53	48.5 ± 28.7	48.0 (23.0-72.0)
	$mitoVO_{2\_max}$	[mm Hg/s]	49	3.2 ± 3.4	2.5 (0.8-3.9)
	Lactate	mmol / L	50	2.2 ± 2.0	1.6 (1.2-2.3)
	$ScvO_2$	%	14	77 ± 10.2	80.5 (73.0-82.5)
8-11hr	$mitoPO_{2\_baseline}$	mm Hg	26	44.1 ± 36.1	39.4 (11.1-69.1)
	$mitoVO_{2\_max}$	[mm Hg/s]	24	2.6 ± 3.0	1.7 (0.1-3.5)
	Lactate	mmol / L	26	2.3 ± 1.8	1.5 (1.3-2.8)
	$ScvO_2$	%	8	78.1 ± 8.2	80.0 (73.8-84.0)
12-15hr	$mitoPO_{2\_baseline}$	mm Hg	15	69.1 ± 41.3	68.0 (39.0-92.0)
	$mitoVO_{2\_max}$	[mm Hg/s]	12	2.6 ± 1.8	2.2 (1.6-3.2)
	Lactate	mmol / L	14	1.9 ± 1.5	1.6 (1.2-1.8)
	$ScvO_2$	%	6	79.0 ± 5.9	81.0 (73.5-83.5)
16-19hr	$mitoPO_{2\_baseline}$	mm Hg	11	73.5 ± 49.7	62.3 (39.7-80.7)
	$mitoVO_{2\_max}$	[mm Hg/s]	8	3.5 ± 3.0	3.7 (0.6-5.8)
	Lactate	mmol / L	9	1.6 ± 0.5	1.6 (1.1-2.1)
	$ScvO_2$	%	5	76.8 ± 10.2	74.0 (67.5-87.5)
20-24hr	$mitoPO_{2\_baseline}$	mm Hg	15	58.8 ± 32.6	62.0 (28.3-80.3)
	$mitoVO_{2\_max}$	[mm Hg/s]	15	5.4 ± 5.1	3.4 (2.3-6.0)
	Lactate	mmol / L	11	2.3 ± 1.7	1.7 (1.2-2.8)
	$ScvO_2$	%	4	79.0 ± 6.4	81.0 (72.3-83.4)

IQR = interquartile range; $mitoPO_{2\_baseline}$ = baseline mitochondrial oxygen tension; $mitoVO_{2\_max}$ = maximum oxygen consumption; SD = standard deviation; $ScvO_2$ = central venous oxygen saturation

In 31 of the total 173 dynamic $mitoPO_2$ measurements, no $mitoVO_2$ could be induced (no decrease in $mitoPO_2$ after applying pressure) (**Table 2**). In 11 of these dynamic $mitoPO_2$ measurements, the $mitoPO_{2\_baseline}$ was extremely low (< 10 mm Hg). In the remaining 20 dynamic $mitoPO_2$ measurements, no $mitoVO_2$ could be induced despite a $mitoPO_{2\_baseline}$ ranging from 10 mm Hg to 101 mm Hg (**APPENDIX IV**).

Longitudinal analysis

The results of the longitudinal analysis estimating the association between lactate or $ScvO_2$ and the mitochondrial parameters are represented in **Table 3**. When adjusted for confounding variables, a significant association was found between $mitoPO_{2\_baseline}$ and lactate. Higher $mitoPO_{2\_baseline}$ levels were significantly associated with lower lactate levels (β = -0.002744, p = 0.023) (**Figure 8**). For an increase in 1 mm Hg in $mitoPO_{2\_baseline}$, there is a decrease of 0.002744 mmol/L in lactate. However, no significant association was found between lactate and $mitoVO_{2\_max}$ and $ScvO_2$ and the mitochondrial parameters (**Table 3**).

Table 3: Longitudinal analysis of lactate / $ScvO_2$ and mitochondrial parameters

Dependent variable	Covariate	β	95% CI	p value
Lactate	$mitoPO_{2\_baseline}$*	-0.002744	-0.005108 – -0.000381	**0.023**
	$mitoVO_{2\_max}$*	0.007605	-0.016031 – 0.031242	0.525
$ScvO_2$	$mitoPO_{2\_baseline}$*	-0.020925	-0.097802 – 0.055953	0.587
	$mitoVO_{2\_max}$*	0.021312	-505169 – 0.547793	0.935

CI = confidence interval; $mitoPO_{2\_baseline}$ = baseline mitochondrial oxygen tension; $mitoVO_{2\_max}$ = maximum oxygen consumption; $ScvO_2$ = central venous oxygen saturation
**Corrected for age, gender, sepsis source and APACHE score*

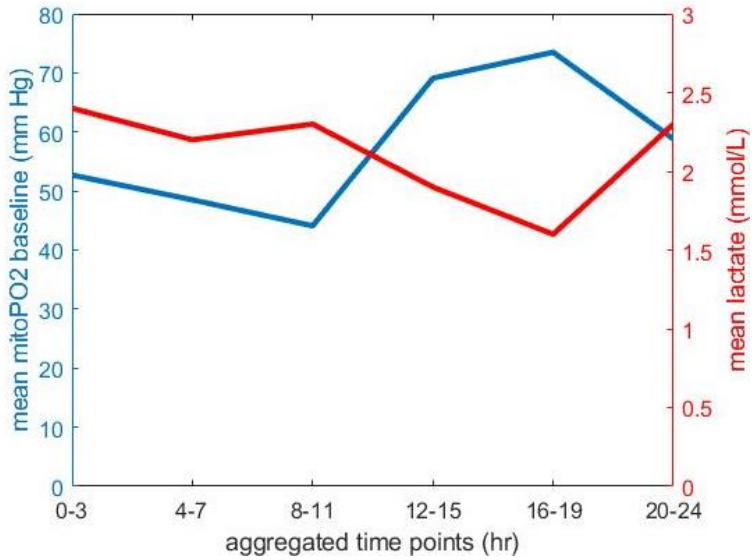

Figure 8: The course of mean lactate and mean baseline mitochondrial oxygen tension ($mitoPO_{2\_baseline}$) over time

Table 4 shows the results of the longitudinal analysis for the association between the $mitoPO_{2\_baseline}$ levels of the $mitoPO_{2\_baseline}$ groups and $mitoVO_{2\_max}$. Higher $mitoPO_{2\_baseline}$ levels were significantly associated with higher $mitoVO_{2\_max}$ in the low $mitoPO_{2\_baseline}$ group (β = 0.103822, p < 0.001) (**Figure 9).** However, no significant association was found between $mitoVO_{2\_max}$ and $mitoPO_{2\_baseline}$ in the other two $mitoPO_{2\_baseline}$ groups.

Table 4 Longitudinal analysis of $mitoPO_{2\_baseline}$ groups and $mitoVO_{2\_max}$

Dependent variable	Covariate	β	95% CI	p value
$mitoVO_{2\_max}$	$mitoPO_{2\_baseline\ low}$ *	0.103822	0.050116 – 0.157528	**<0.001**
	$mitoPO_{2\_baseline\ medium}$ *	-0.042870	-0.175930 – 0.090190	0.518
	$mitoPO_{2\_baseline\ high}$ *	-0.010023	-0.043914 – 0.023867	0.551

CI = confidence interval; $mitoPO_{2\_baseline}$ = baseline mitochondrial oxygen tension; $mitoVO_{2\_max}$ = maximum oxygen consumption
Low = $mitoPO_{2\_baseline}$ 0-40 mm Hg
Medium = $mitoPO_{2\_baseline}$ 41-62.3 mm Hg
High = $mitoPO_{2\_baseline}$ >62.3 mm Hg
**Corrected for age, gender, sepsis source and APACHE score*

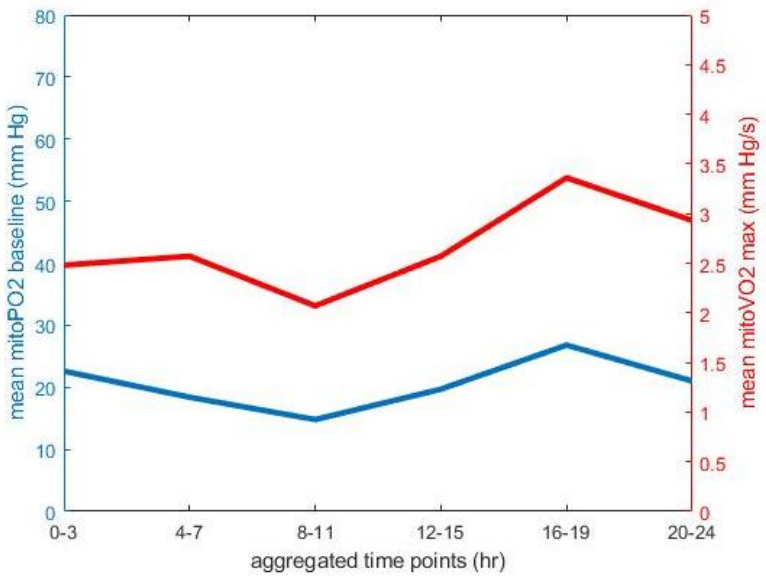

Figure 9: The course of mean maximum oxygen consumption ($mitoVO_{2\_max}$) and mean baseline mitochondrial oxygen tension ($mitoPO_{2\_baseline}$) over time for the low $mitoPO_{2\_baseline}$ group.

Discussion

This study developed an analysis method to derive a measure for oxygen consumption from dynamic mitoPO$_2$ measurements. Using this dynamic mitochondrial parameter, we investigated the association between the macrocirculation and the mitochondrial oxygenation, in particular mitoPO$_2$ and mitoVO$_2$, and the association between these two mitochondrial parameters in critically ill patients with sepsis.The results of this study showed that higher mitoPO$_{2_baseline}$ levels were significantly associated with lower lactate levels. Despite that mitoVO$_2$ could not be induced during all the dynamic mitoPO$_2$ measurements, mitoPO$_2$ levels of the low mitoPO$_{2_baseline}$ group were significantly associated with higher mitoVO$_2$ rates. This suggests that mitochondria with low mitoPO$_{2_baseline}$ levels are in stress and switch to anaerobic metabolism. The situation will exacerbate when the microcirculatory oxygen supply is temporarily blocked because the mitochondria with low mitoPO$_{2_baseline}$ levels consume the present oxygen faster compared to the mitochondria with higher mitoPO$_{2_baseline}$ levels. Interestingly, oxygen consumption could not be induced during some dynamic mitoPO$_2$ measurements despite sufficient oxygen supply. This observation may support the hypothesis that mitochondrial dysfunction plays a role in the pathogenesis of sepsis.

Interpretation

Association between the macrocirculation and mitochondrial oxygenation

The early physiologic response in sepsis is characterized by tissue hypoxia as a consequence of hemodynamic perturbations that create an imbalance between systemic oxygen supply and consumption (33-34). Anaerobic metabolism ensues when mitochondrial oxygen consumption is impaired leading to lactate production (35). Impaired mitochondrial consumption can be the consequence of a critical level of mitochondrial oxygen supply or mitochondrial dysfunction. Lactate is produced at the cellular level and therefore a direct indicator of the oxygen balance, the balance between oxygen supply and oxygen consumption. Although the study found a significant association between lactate and mitoPO$_{2_baseline}$, no association was found between lactate and mitoVO$_{2_max}$. This result can be explained by the fact that mitoPO$_2$, like lactate, is a direct indicator of the oxygen balance but at mitochondrial the level. MitoPO$_2$ is the resultant of the amount of oxygen diffusing into the mitochondria and the amount of oxygen consumed by the mitochondria. In contrast, mitoVO$_2$ only reflects the oxygen consumption by the mitochondria.

Compared to lactate, no association was found between ScvO$_2$ and the two mitochondrial parameters. ScvO$_2$ is the level of oxygen saturation in the blood after transport of oxygen to the cells, measured from the vena cava superior. In contrast to lactate, ScvO$_2$ gives only a global indication of the oxygen balance at the cellular level, indicating how much oxygen remains after delivery to the cells. A ScvO$_2$ of less than 70% is indicative of insufficient oxygen supply and/or increased oxygen consumption (36). However, normalized ScvO$_2$ values after resuscitation do not reflect adequate tissue oxygenation by definition since the cells may not be able to use the oxygen due to possible microcirculatory or mitochondrial dysfunction (37). ScvO$_2$ and the mitochondrial parameters are measured at different levels and their relationship depends on several factors, such as the condition of the microcirculation. This may explain that no association was found between ScvO$_2$ and the mitochondrial parameters.

Association between the mitochondrial oxygenation and oxygen consumption

The current study found that the mitoPO$_2$ levels of the low mitoPO$_{2_baseline}$ group were significantly associated with higher mitoVO$_2$ rates. Mitochondria with low oxygen levels are most likely 'not happy' and in stress. When the microcirculatory oxygen supply was acutely blocked, the situation exacerbated because these mitochondria consumed the present oxygen faster leading to even lower oxygen levels in a short time. This suggests that the mitochondria with lower mitoPO$_{2_baseline}$ levels are directly affected by the acute cessation of the microcirculatory oxygen supply. However, the mitoPO$_2$ levels of the 'happy' mitochondria, the medium and high mitoPO$_{2_baseline}$ group, were not associated with the mitoVO$_2$ rate. This indicates that these 'happy' mitochondria have enough reserves and are not directly affected by the acute cessation of the microcirculatory oxygen supply.

However, one unanticipated finding was that mitoVO$_2$ could not be induced during some dynamic mitoPO$_2$ measurements. In a part of these dynamic mitoPO$_2$ measurements, the mitoPO$_{2_baseline}$ was very low (< 10 mm Hg). These mitochondria initiate cell death through apoptosis in response to the low oxygen levels (38). In the other part of these dynamic mitoPO$_2$ measurements without inducible mitoVO$_2$, the mitoPO$_{2_baseline}$ varied between 10 mm Hg and 101 mm Hg. These mitochondria are in shutdown and do not respond to the acute cessation of the microcirculatory oxygen supply. This finding is also observed in the study of Neu et.al. which tested the feasibility of the COMET measurements in critically ill patients with sepsis (27). They excluded the dynamic mitoPO$_2$ measurements without inducible mitoVO$_2$ for further analysis. This may be the reason that Neu et.al. calculated higher values for mitoVO$_{2_max}$ in critically ill septic patients compared to our study (27).

Insufficient oxygen consumption despite sufficient oxygen supply is defined as cytopathic hypoxia (12-14). In the classic view, oxygen consumption is unaffected by oxygen levels until mitoPO$_2$ decreases below 2 to 3 mm Hg, because oxidative phosphorylation has a high affinity for oxygen (39-42). However, in the modern view, oxygen availability at much higher mitoPO$_2$ levels than 2-3 mm Hg directly influences oxygen consumption and function by a mechanism called oxygen conformance. Oxygen conformance is a cellular metabolic adaption mechanism in which mitochondrial oxygen consumption is downregulated in response to a decline in oxygen availability (28, 43). Oxygen conformance can occur over a wide mitoPO$_2$ range starting below 70 mm Hg (28). Besides oxygen conformance, mitochondrial dysfunction due to direct damage could also contribute to cytopathic hypoxia. This mitochondrial dysfunction might be caused by oxygen stress, medication and inflammation-induced metabolic changes, which are part of the pathogenesis and treatment of sepsis (44). However, if cytopathic hypoxia, either caused by mitochondrial dysfunction or as part of a cellular adaption mechanism, exists in the presence of a normalized macro- and microcirculation, this would have an impact on the understanding of resuscitation medicine. Findings from animal studies with endotoxemic models of acute critical illness provide evidence that this might be the case. Harms et. al. and Wefers-Bettink et. al. observed a decreased oxygen consumption in endotoxemic rats after restoring mitochondrial oxygenation to baseline levels by fluid resuscitation (45-46). If this is the case, attempts to improve clinical outcomes in patients with sepsis by optimizing systemic hemodynamic parameters and microcirculatory perfusion are doomed to failure. Instead, the focus should shift to pharmacological drugs to the development of pharmacological drugs to restore normal mitochondrial function.

Limitations

Although the COMET monitor is the first clinical device that provides insight into the oxygen balance at the mitochondrial level, the used technology has some limitations. After application of the ALA patch, at least four hours is needed to synthesize a suitable PpIX concentration in the mitochondria to enable mitoPO$_2$ measurements. This makes that the COMET monitor is not directly applicable when a patient with sepsis is admitted to the ICU. This results in a lack of data for the first four hours which could be relevant for treatment decisions. Moreover, the presence of edema in septic patients may affect the COMET measurements, because the measurement depth is limited to the epidermis layer (0.3-0.6 mm) since the stratum corneum is a barrier for topical ALA skin penetration (47). Lower mitoPO$_2$ values have been measured in more hydrated (i.e. with edema) patients with sepsis (27). The study protocol is also subject to certain limitations. First of all, multiple dynamic mitoPO$_2$ measurements instead of one dynamic mitoPO$_2$ measurement have to be performed at each predefined time point to increase the reliability of the results. Furthermore, future dynamic mitoPO$_2$ measurements have to be performed in a strictly standardized way. Adequate detection of a mitoPO$_2$ baseline is essential to select the starting point of the oxygen consumption phase. Besides, each part of the dynamic mitoPO$_2$ measurement (baseline, pressure, pressure release) must be performed for a fixed time to determine reliable mitochondrial parameters. Finally, the generalizability of the results is limited by the relatively small number of patients (n = 41) and the single academic center design of the study.

Future research

This study poses a first step toward the assessment of mitochondrial oxygenation in critically ill patients with sepsis. The results of this study contribute to our understanding of the mitochondrial function and the association between the macrocirculation and mitochondrial oxygenation in sepsis. Future studies with larger cohorts are needed to determine mitoPO_2's and mitoVO_2's clinical and diagnostic applicability in septic patients. Moreover, these future studies may also focus on the ascending part of the dynamic mitoPO_2 measurement to derive a measure for mitochondrial oxygen delivery (mitoDO_2). MitoDO_2 may be an interesting parameter of reoxygenation capacity as a surrogate marker for impaired microcirculation. Besides, future studies could assess whether current resuscitation procedures aimed at the optimization of the systemic hemodynamic parameters of a patient are actually improving the patient's microcirculatory and mitochondrial function. Therefore, future studies have to include the assessment of microcirculatory function by using bedside tools that allow direct visualization of the microcirculation. Furthermore, healthy volunteers should be measured to generate normal values for the mitochondrial parameters. The ultimate goal is to achieve oxygen hemostasis by current resuscitation procedures and/or additional mitochondrial target drugs and thus maintaining the mitochondrial parameters within the normal range.

References

1. Ince C. Hemodynamic coherence and the rationale for monitoring the microcirculation. Crit Care. 2015;19 Suppl 3:S8
2. van Genderen ME, Klijn E, Lima A, de Jonge J, Sleeswijk Visser S, Voorbeijtel J, et al. Microvascular perfusion as a target for fluid resuscitation in experimental circulatory shock. Crit Care Med. 2014;42(2):e96-e105.
3. Trzeciak S, McCoy JV, Phillip Dellinger R, Arnold RC, Rizzuto M, Abate NL, et al. Early increases in microcirculatory perfusion during protocol-directed resuscitation are associated with reduced multi-organ failure at 24 h in patients with sepsis. Intensive Care Med. 2008;34(12):2210-7.
4. Sakr Y, Dubois MJ, De Backer D, Creteur J, Vincent JL. Persistent microcirculatory alterations are associated with organ failure and death in patients with septic shock. Crit Care Med. 2004;32(9):1825-31.
5. Edul VS, Enrico C, Laviolle B, Vazquez AR, Ince C, Dubin A. Quantitative assessment of the microcirculation in healthy volunteers and in patients with septic shock. Crit Care Med. 2012;40(5):1443-8.
6. Ince C, Sinaasappel M. Microcirculatory oxygenation and shunting in sepsis and shock. Crit Care Med. 1999;27(7):1369-77.
7. Donati A, Damiani E, Domizi R, et.al. Alteration of the sublingual microvascular glycocalyx in critically ill patients. Microvasc Res. 2013;90:86-9.
8. Klijn E, Uil Den CA, Bakker J, et.al. The heterogeneity of the microcirculation in critical illness. Clin Chest Med. 2008;29:643-55.
9. Rivers EP, Jaehne AK, Eichhorn-Wharry L, Brown S, Amponsah D. Fluid therapy in septic shock. Curr Opin Crit Care. 2010;16(4):297-308.
10. Ospina-Tascon G, Neves AP, Occhipinti G, Donadello K, Buchele G, Simion D, et al. Effects of fluids on microvascular perfusion in patients with severe sepsis. Intensive Care Med. 2010;36(6):949-55.
11. Hernandez G, Bruhn A, Castro R, Regueira T. The holistic view on perfusion monitoring in septic shock. Curr Opin Crit Care. 2012;18(3):280-6.
12. Fink MP. Cytopathic hypoxia. Is oxygen use impaired in sepsis as a result of an acquired intrinsic derangement in cellular respiration? Crit Care Clin. 2002;18(1):165-75.
13. Fink MP. Cytopathic hypoxia. Mitochondrial dysfunction as mechanism contributing to organ dysfunction in sepsis. Crit Care Clin. 2001;17(1):219-37.
14. Fink M. Cytopathic hypoxia in sepsis. Acta Anaesthesiol Scand Suppl. 1997;110:87-95.
15. Kohoutova M, Dejmek J, Tuma Z, Kuncova J. Variability of mitochondrial respiration in relation to sepsis-induced multiple organ dysfunction. Physiol Res. 2018;67(Suppl 4):S577-S92.
16. Jeger V, Djafarzadeh S, Jakob SM, Takala J. Mitochondrial function in sepsis. Eur J Clin Invest. 2013;43(5):532-42.
17. Mik EG, Stap J, Sinaasappel M, Beek JF, Aten JA, van Leeuwen TG, et al. Mitochondrial PO2 measured by delayed fluorescence of endogenous protoporphyrin IX. Nat Methods. 2006;3(11):939-45.
18. Mik EG, Johannes T, Zuurbier CJ, Heinen A, Houben-Weerts JH, Balestra GM, et al. In vivo mitochondrial oxygen tension measured by a delayed fluorescence lifetime technique. Biophys J. 2008;95(8):3977-90.
19. Mik EG, Ince C, Eerbeek O, Heinen A, Stap J, Hooibrink B, et al. Mitochondrial oxygen tension within the heart. J Mol Cell Cardiol. 2009;46(6):943-51.
20. Bodmer SI, Balestra GM, Harms FA, Johannes T, Raat NJ, Stolker RJ, et al. Microvascular and mitochondrial PO(2) simultaneously measured by oxygen-dependent delayed luminescence. J Biophotonics. 2012;5(2):140-51.

21. Harms FA, de Boon WM, Balestra GM, Bodmer SI, Johannes T, Stolker RJ, et al. Oxygen-dependent delayed fluorescence measured in skin after topical application of 5-aminolevulinic acid. J Biophotonics. 2011;4(10):731-9.
22. Harms FA, Bodmer SI, Raat NJ, Stolker RJ, Mik EG. Validation of the protoporphyrin IX-triplet state lifetime technique for mitochondrial oxygen measurements in the skin. Opt Lett. 2012;37(13):2625-7.
23. Harms FA, Voorbeijtel WJ, Bodmer SI, Raat NJ, Mik EG. Cutaneous respirometry by dynamic measurement of mitochondrial oxygen tension for monitoring mitochondrial function in vivo. Mitochondrion. 2013;13(5):507-14.
24. Ubbink R, Bettink MAW, Janse R, Harms FA, Johannes T, Munker FM, et al. A monitor for Cellular Oxygen METabolism (COMET): monitoring tissue oxygenation at the mitochondrial level. J Clin Monit Comput. 2017;31(6):1143-50.
25. Baumbach P, Neu C, Derlien S, Bauer M, Nisser M, Buder A, et al. A pilot study of exercise-induced changes in mitochondrial oxygen metabolism measured by a cellular oxygen metabolism monitor (PICOMET). Biochim Biophys Acta Mol Basis Dis. 2019;1865(4):749-58.
26. van Diemen MPJ, Berends CL, Akram N, Wezel J, Teeuwisse WM, Mik BG, et al. Validation of a pharmacological model for mitochondrial dysfunction in healthy subjects using simvastatin: A randomized placebo-controlled proof-of-pharmacology study. Eur J Pharmacol. 2017;815:290-7.
27. Neu C, Baumbach P, Plooij AK, Skitek K, Gotze J, von Loeffelholz C, et al. Non-invasive Assessment of Mitochondrial Oxygen Metabolism in the Critically Ill Patient Using the Protoporphyrin IX-Triplet State Lifetime Technique-A Feasibility Study. Front Immunol. 2020;11:757.
28. Mik EG. Special article: measuring mitochondrial oxygen tension: from basic principles to application in humans. Anesth Analg. 2013;117(4):834-46.
29. Layer G, Reichelt J, Jahn D, Heinz DW. Structure and function of enzymes in heme biosynthesis. Protein Sci. 2010;19(6):1137-61.
30. Singer M, Deutschman CS, Seymour CW. The Third International Consensus Definitions for Sepsis and Septic Shock (Sepsis-3). JAMA 2016;315:801-10.
31. Kreyszig, E. "Principal Normal, Curvature, Osculating Circle." §12 in Differential Geometry. New York: Dover;1991. p. 34-36.
32. Akaike H. A new look at the statistical model identification. IEEE Trans Autom Control. 1974;19(6):716–23.
33. Nguyen HB, Jaehne AK, Jayaprakash N, et al. Early goal-directed therapy in severe sepsis and septic shock: insights and comparisons to ProCESS, ProMISe, and ARISE. Crit Care 2016;20:160.
34. Rivers E, Nguyen B, Havstad S, et al. Early goal-directed therapy in the treatment of severe sepsis and septic shock. N Engl J Med 2001;345:1368-77.
35. Kasnitz P, Druger GL, Yorra F, Simmons DH. Mixed venous oxygen tension and hyperlactatemia. Survival in severe cardiopulmonary disease. JAMA. 1976;236(6):570–4.
36. Wittayachamnankul B, Chentanakij B, Sruamsiri K, Chattipakorn N. The role of central venous oxygen saturation, blood lactate, and central venous-to-arterial carbon dioxide partial pressure difference as a goal and prognosis of sepsis treatment. J Crit Care 2016;36:223-9.
37. Rivers EP, Elkin R, Cannon CM. Counterpoint: should lactate clearance be substituted for central venous oxygen saturation as goals of early severe sepsis and septic shock therapy? No. Chest 2011;140:1408-13; discussion 13-9.
38. Snyder CM, Chandel NS. Mitochondrial regulation of cell survival and death during low-oxygen conditions. Antioxid Redox Signal. 2009;11(11):2673-83.
39. Jones DP, Mason HS. Gradients of O2 concentration in hepatocytes. J Biol Chem. 1978;253(14):4874-80.
40. Longmuir IS. Respiration rate of rat-liver cells at low oxygen concentrations. Biochem J. 1957;65(2):378-82.

41. Wilson DF, Erecinska M, Drown C, Silver IA. The oxygen dependence of cellular energy metabolism. Arch Biochem Biophys. 1979;195(2):485-93.
42. Wilson DF, Rumsey WL, Green TJ, Vanderkooi JM. The oxygen dependence of mitochondrial oxidative phosphorylation measured by a new optical method for measuring oxygen concentration. J Biol Chem. 1988;263(6):2712-8.
43. Arthur PG, Giles JJ, Wakeford CM. Protein synthesis during oxygen conformance and severe hypoxia in the mouse muscle cell line C2C12. Biochim Biophys Acta. 2000;1475(1):83-9.
44. Wefers Bettink MA, Arbous MS, Raat NJ, Mik EG. Mind the mitochondria! J emerg Crit Care Med 2019;3:45.
45. Harms FA, Bodmer SI, Raat NJ, Mik EG. Non-invasive monitoring of mitochondrial oxygenation and respiration in critical illness using a novel technique. Crit Care. 2015;19:343.
46. Wefers Bettink MA, Harms FA, Dollee N, Specht PAC, Raat NJH, Schoonderwoerd GC, et al. Non-invasive versus ex vivo measurement of mitochondrial function in an endotoxemia model in rat: Toward monitoring of mitochondrial therapy. Mitochondrion. 2020;50:149-57.
47. Wachowska M, Muchowicz A, Firczuk M, Gabrysiak M, Winiarska M, Wanczyk M, et al. Aminolevulinic Acid (ALA) as a Prodrug in Photodynamic Therapy of Cancer. Molecules. 2011;16(5):4140-64.

APPENDIX I

*The self-developed MATLAB script used for data preparation and calculation of the mitochondrial parameters (Analysis_method.*m)*

Step 1: Load data from the Excel file

```
clear all; close all; clc;

% Fill in the path of the folder where the datafile is located
path = 'C:\Users\ … ';

% Fill in the folder name of the patient folder
patient = '…';

% Fill in the name of the Excel file
timepoint = ['…'];

% Retrieve mitoPO₂, SNR and t from the Excel file
[MitoPO2, SNR, t] = load_data(patient, timepoint, path);

% Save raw MitoPO2 data
MitoPO2_raw = MitoPO2;
```

Step 2: Interpolate mitoPO₂ samples with SNR < 5

Since the COMET monitor operates reliably at SNR ≥ 5, only mitoPO₂ samples with an SNR ≥ 5 were analyzed. Therefore, one, two or three consecutive mitoPO₂ samples of a dynamic mitoPO₂ measurement with an SNR < 5 were interpolated.

```
[MitoPO2, t] = cut_lowSNR(MitoPO2, SNR, t);

function [MitoPO2, t] = cut_lowSNR(MitoPO2, SNR, t)
for k = 2:length(SNR)-1
    if SNR(k) < 5 && SNR(k+1) >= 5
        MitoPO2(k) = round((MitoPO2(k-1) +
MitoPO2(k+1))/2);
    end
    if SNR(k) < 5 && SNR(k+1) < 5
        MitoPO2(k) = round((MitoPO2(k-1) +
MitoPO2(k+2))/2);
        MitoPO2(k+1) = round((MitoPO2(k) +
MitoPO2(k+2))/2);
    end
       if SNR(k) < 5 && SNR(k+1) < 5 && SNR(k+2) < 5
       MitoPO2(k) = round((MitoPO2(k-1) +
MitoPO2(k+3))/2);
       MitoPO2(k+1) = round((MitoPO2(k) +
MitoPO2(k+3))/2);
       MitoPO2(k+2) = round((MitoPO2(k+1) +
MitoPO2(k+3))/2);
   end
end
```

```
% Plot raw mitoPO2 signal, mitoPO2 signal after
interpolation and SNR in one figure
figure(1)
hold on
% Threshold line SNR = 5
yline(5)
plot(t,MitoPO2_raw)
plot(t, MitoPO2)
plot(t, SNR)
legend('SNR = 5', 'Raw mitoPO2 signal', 'Raw mitoPO2
signal after interpolation', 'SNR')
xlabel('Time (s)','FontSize',16);
ylabel('MitoPO2 (mm Hg)','FontSize',16);
```

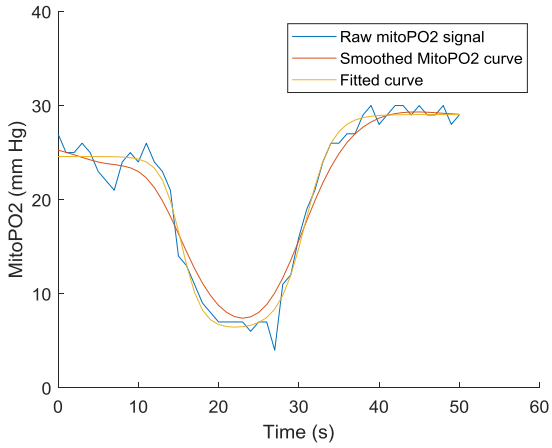

Step 3: Smooth raw mitoPO₂ signal by Gaussian filter to estimate the initial parameters of the sigmoid function

Smoothing is a process by which data points are averaged with their neighbours. A Gaussian-weighted moving average filter uses a fixed window, consisting of a kernel that represents the shape of a Gaussian (normal distribution) curve. This window slices down the length of the raw mitoPO₂ signal to compute an average over the neighbouring mitoPO₂ samples within each window. The window size could be specified by the smoothing factor 'x'. For smoothing factor 'x', the moving average window size consists of 100*'x' percent of the samples of the input data.

```
% Smooth raw mitoPO2 signal
smoothedData =
smoothdata(MitoPO2,'gaussian','SmoothingFactor',0.4);

% Visualize results
clf
plot(MitoPO2,'Color',[109 185
226]/255,'DisplayName','Input data')
hold on
plot(smoothedData,'Color',[0 114
189]/255,'LineWidth',1.5,...
    'DisplayName','Smoothed data')
hold off
legend
legend('Raw mitoPO2 signal', 'Smoothed MitoPO2 curve')
xlabel('Time (s)','FontSize',16);
ylabel('MitoPO2 (mm Hg)','FontSize',16);
```

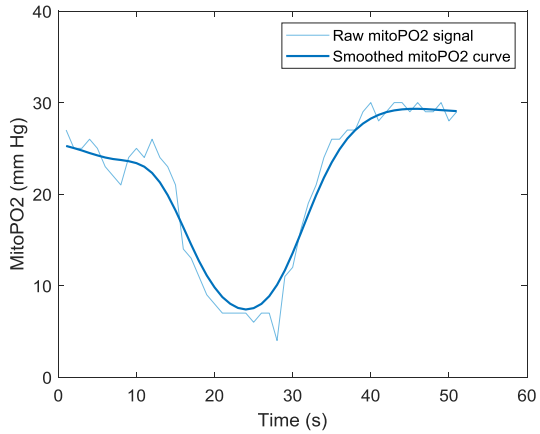

Step 4: Sigmoid function

The smoothed mitoPO₂ curve and its first derivative were used to estimate the initial parameters of the two complementary sigmoid functions. If the dynamic mitoPO₂ measurement did not contain an ascending part, only a single sigmoid function was used to fit the descending part of the raw mitoPO₂ signal.

```
% Define values for the initial parameters of the
sigmoid function

% K1 starting point = mean of the first 5 mitoPO2
samples of the dynamic mitoPO2 measurement
K1_int = mean(MitoPO2(1:5));
% [Lower boundary upper boundary starting point]
K1 = [1 150 K1_int];

% K2 starting point = mean of the last 5 mitoPO2
samples of the dynamic mitoPO2 measurement
K2_int = mean(MitoPO2((end-5):end));
K2 = [1 150 K2_int];

% First derivative of smoothed mitoPO2 curve
derivative1 = diff(smoothedData);

% B1 starting point = minimum of the first derivative
of the smoothed mitoPO2 curve
[B1_int, ind_B1_int] = min(derivative1);
B1 = [B1_int-10 0 B1_int];

% M1 starting point = time index of B1
M1 = [ind_B1_int-20 ind_B1_int+20 ind_B1_int];

% B2 starting point = maximum  of the first derivative
of the smoothed mitoPO2 curve
[B2_int, ind_B2_int] = max(derivative1);
B2 = [0 10 B2_int];

% M2 starting point = time index of B2
M2 = [ind_B2_int-20 ind_B2_int+20 ind_B2_int];
```

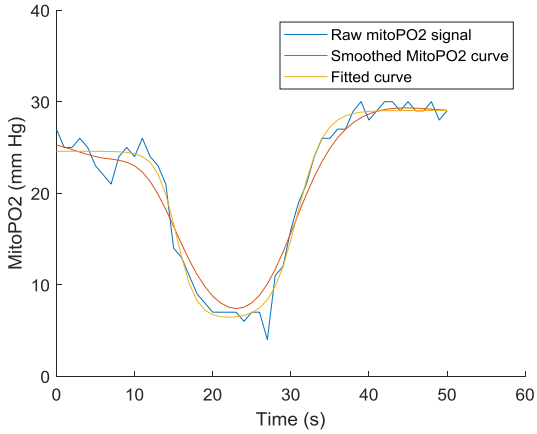

```
% Z starting point = minimum value of raw MitoPO2
signal
Z_int = min(MitoPO2);
Z = [0 Z_int+5 Z_int];

% Define fit function type
ft = fittype( '(K1./(1+exp(-B1*(x-M1))))+(K2./(1+exp(-
B2*(x-M2))))+Z', 'independent', 'x', 'dependent', 'y'
);
% Define fit options (upper/lower boundaries and
starting  points for parameter estimates)
fo=fitoptions('gauss2','Lower',[B1(1) B2(1) K1(1)
K2(1) M1(1) M2(1) Z(1)],'Upper',[B1(2) B2(2) K1(2)
K2(2) M1(2) M2(2) Z(2)],'StartPoint',[B1(3) B2(3)
K1(3) K2(3) M1(3) M2(3) Z(3)]);

% Parameter estimation using fit function
[fitresult, gof] = fit(t, MitoPO2, ft, fo);

% Create sigmoid fit
fit1 = fitresult(t);

% If the dynamic mitoPO2 measurement did not contain
an ascending part, only a single sigmoid function was
used to fit the descending part of the raw mitoPO2
signal
% Define fit function type
ft = fittype( '(K1./(1+exp(-B1*(x-M1))))+Z',
'independent', 'x', 'dependent', 'y' );
% Define fit options (upper/lower boundaries and
starting points for parameter estimates)
fo = fitoptions('gauss2','Lower',[B1(1) K1(1) M1(1)
Z(1)],'Upper',[B1(2) K1(2) M1(2)
Z(2)],'StartPoint',[B1(3) K1(3) M1(3) Z(3)]);
% Parameter estimation using fit function
[fitresult, gof] = fit(t, MitoPO2, ft, fo);
% Create sigmoid fit
fit1 = fitresult(t);
```

```
% Plot raw mitoPO2 signal, smoothed MitoPO2 curve and
fitted curve in one figure
figure(3);
hold on;
plot(t,MitoPO2);
plot(t,smoothedData);
plot(t,fit1);
legend('Raw mitoPO2 signal', 'Smoothed MitoPO2 curve',
'Fitted curve')
xlabel('Time (s)','FontSize',16);
ylabel('MitoPO2 (mm Hg)','FontSize',16);
```

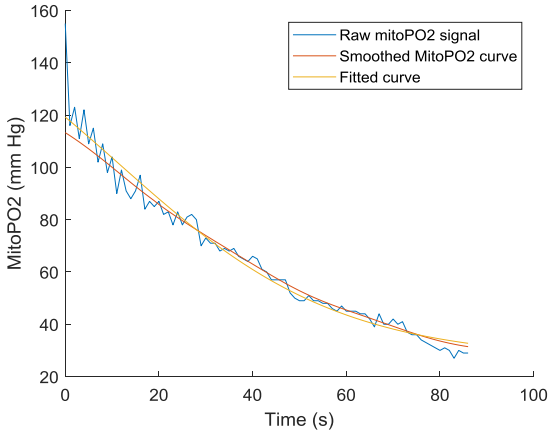

Step 5: Optimization of the sigmoid function

To optimize the first fitted curve, the initial parameters of the sigmoid function were re-estimated based on the first derivative of the first fitted curve creating a second optimized fitted curve.

```
K1_int = mean(MitoPO2(1:5));
K1 = [1 150 K1_int];

K2_int = mean(MitoPO2((end-5):end));
K2 = [1 150 K2_int];

% First derivative of fitted curve
derivative2 = diff(fit1);

% B11 starting point = minimum of the first derivative
of the fitted curve
[B11_int, ind_B11_int] = min(derivative2);
B11 = [B11_int-10 0 B11_int];

% M11 starting point = time index of B11
M11 = [ind_B11_int-20 ind_B11_int+20 ind_B11_int];

% B22 starting point = maximum of the first derivative
of the fitted curve
[B22_int, ind_B22_int] = max(derivative2);
B22 = [0 10 B22_int];

% M22 starting point = time index of B22
M22 = [ind_B22_int-20 ind_B22_int+20 ind_B22_int];

Z_int = min(MitoPO2);
Z = [0 Z_int+5 Z_int];

% Define fit function type
ft1 = fittype( '(K1./(1+exp(-B11*(x-
M11))))+(K2./(1+exp(-B22*(x-M22))))+Z', 'independent',
'x', 'dependent', 'y' );
% Define fit options (upper/lower boundaries and
starting points for parameter estimates)
fo1 = fitoptions('gauss2','Lower',[B11(1) B22(1) K1(1)
K2(1) M11(1) M22(1) Z(1)],'Upper',[B11(2) B22(2) K1(2)
K2(2) M11(2) M22(2) Z(2)],'StartPoint',[B11(3) B22(3)
K1(3) K2(3) M11(3) M22(3) Z(3)]);
% Parameter estimation using fit function
[fitresult1, gof1] = fit(t, MitoPO2, ft1, fo1);
% Create second optimized sigmoid fit
fit2 = fitresult1(t);
% If the dynamic mitoPO2 measurement did not contain
an ascending part, only a single sigmoid function was
used to fit the descending part of the raw mitoPO2
signal
% Define fit function type
ft1 = fittype( '(K1./(1+exp(-B1*(x-M1))))+Z',
'independent', 'x', 'dependent', 'y' );
% Define fit options (upper/lower boundaries and
starting points for parameter estimates)
fo1 = fitoptions('gauss2','Lower',[B11(1) K1(1) M11(1)
Z(1)],'Upper',[B11(2) K1(2) M11(2)
Z(2)],'StartPoint',[B11(3) K1(3) M11(3) Z(3)]);
% Parameter estimation using fit function
[fitresult1, gof1] = fit(t, MitoPO2, ft1, fo1);
% Create sigmoid fit
fit2 = fitresult(t);

% Plot raw MitoPO2, smoothed MitoPO2 curve and
optimized fitted curve in one figure
figure(4);
hold on;
plot(t, MitoPO2);
plot(t, smoothedData)
plot(t,fit2);
legend('Raw mitoPO2 signal', 'Smoothed MitoPO2 curve',
'Optimized fitted curve')
```

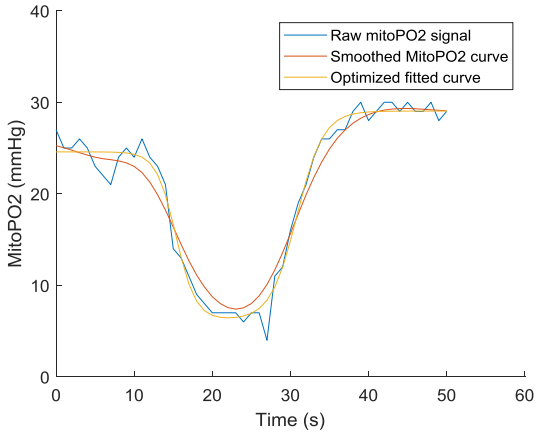

Step 6: Baseline correction

If the optimized fitted curve did not adequately detect the baseline of the dynamic mitoPO$_2$ measurement, the first part of the optimized fitted curve was manually replaced by the first part of the Gaussian smoothed mitoPO$_2$ curve.

```
% No adequate detection of the MitoPO2 baseline by the
optimized fitted curve
% No adequate detection of the MitoPO2 baseline by the
optimized fitted curve
difference = fit2 - smoothedData;
% Difference samples 1 t/m 30
difference_select = difference(1:30);
% Absolute value
difference_select = abs(difference_select);
% Sort values and indices of the difference vector
[values, indices] = sort(difference_select);

% Select index with the smallest difference between
optimized fitted curve and smoothed mitoPO2 curve
index = indices(1);

% Part 1: 1 t/m index = smoothed mitoPO2 curve
a1 = smoothedData(1:index-1);
% Part 2: index t/m end = optimized fitted curve
a2 = fit2(index:length(fit2));
% Create new vector
a = [a1;a2];
% Smooth first part of the created vector (index + 10)
a3 = smooth(a(1:index+10));
% Second part of the created vector
a4 = a(index+11:length(a));
% Result: optimized fitted with adequate baseline
detection (by smoothed mitoPO2 curve)
a =[a3;a4];

% Adequate detection of the MitoPO2 baseline by the
optimized fitted curve (CHOOSE HERE)
a = fit2;
```

```
% Plot raw mitoPO2 signal, smoothed MitoPO2 curve,
optimized fitted curve without baseline correction and
optimized fitted curve with baseline correction in one
figure
figure(5)
hold on;
plot(t,MitoPO2);
plot(t,fit2);
plot(t,a);
legend('Raw mitoPO2 signal', 'Optimized fitted curve
without baseline correction', 'Optimized fitted curve
with baseline correction')
xlabel('Time (s)','FontSize',16);
ylabel('MitoPO2 (mm Hg)','FontSize',16);
```

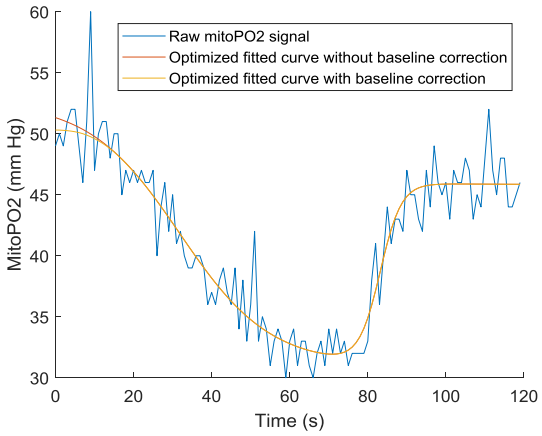

Step 7: Find starting point and endpoint of the descending part of the optimized fitted curve
The starting point and endpoint of the descending part of the optimized fitted curve were determined by the curvature formula. This formula indicates how fast the optimized fitted curve changes direction at each time point.

```
f1 = gradient(a);
f2 = gradient(gradient(a));
% Positive curvature formula (background information
is provided at the end of this APPENDIX)
k1 = f2 ./ (1+f1.^2).^1.5;
% Negative curvature formula
k2 = -1*k1;

[pks1, locs1] = findpeaks(k1);    % Findpeaks in k1

[pks2, locs2] = findpeaks(k2);    % Findpeaks in k2

% Delete negative peaks in k1
del1 = find(pks1<0);
pks1(del1) = [];
locs1(del1) = [];
% Delete negative peaks in k2
del2 = find(pks2<0);
pks2(del2) = [];
locs2(del2) = [];

% Plot 3 subplots:
% 1) Plot raw mitoPO2 signal and optimized fitted
curve in one plot;
% 2) Findpeaks k1;
% 3) Findpeaks k2;

figure(6)
subplot(3,1,1), plot(t, MitoPO2);
hold on
subplot(3,1,1), plot(t, a);
legend('Raw mitoPO2 signal', 'Optimized fitted curve')
xlabel('Time (s)');
ylabel('MitoPO2 (mm Hg)');
set(gca,'Ylim', [0 40], 'YTick', [0:10:40])
set(gca,'Xlim', [0 60], 'XTick', [0:10:60])
subplot(3,1,2), findpeaks(k1)
legend('Findpeaks in positive curvature formula')
xlabel('Time (s)');
set(gca,'Xlim', [0 60], 'XTick', [0:10:60])
subplot(3,1,3), findpeaks(k2);
legend('Findpeaks in negative curvature formula')
xlabel('Time (s)');
set(gca,'Xlim', [0 60], 'XTick', [0:10:60])
```

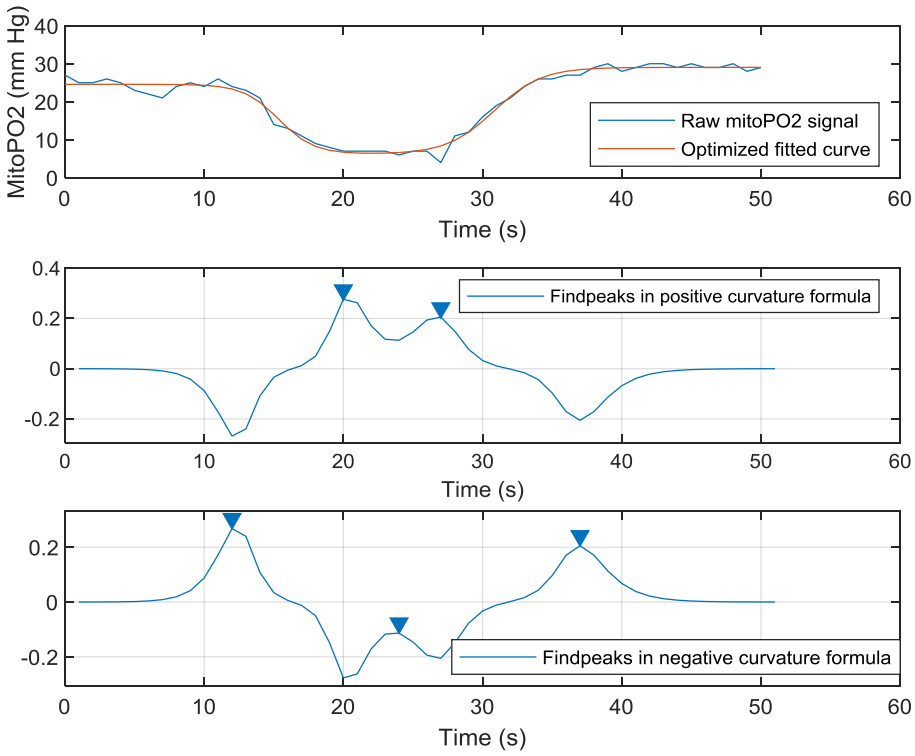
MitoPO2 (mm Hg)
Time (s)
Raw mitoPO2 signal
Optimized fitted curve
Findpeaks in positive curvature formula
Findpeaks in negative curvature formula

Endpoint of the descending part of the optimized fitted curve = MitoVO2_end

```
% First derivative of the optimized fitted curve
with(out) baseline correction
derivative3 = diff(a);
if length(pks1) == 1
% If k1 contains one peak
     derivative4 = derivative3(10:end);
% Cut first 10 datapoints of the first derivative
vector to prevent too early endpoint detection
     X = zeros(1,length(derivative4));
% Create vector X with zeros
     for i = 1:length(derivative4)-1
        if derivative4(i) < 0 && derivative4(i+1) > 0
% Find point: negative to positive derivative, give
this point value 100 in X vector
        X(i) = 100;
        XX = find(X==100);
        MitoVO2_end = XX+10;
        end
end
end

if length(pks1) > 1
% If k1 contains more than one peak
    distance = locs1(2) - locs1(1);
% Distance between the two peaks
    if pks1(1) > 0.1 && pks1(2) > 0.1 && distance > 7
% If these two peaks have both a height of 0.1 and the
distance between these points > 7, MitoVO2_end = peak
1
    MitoVO2_end = locs1(1);
    else
    derivative4 = derivative3(10:end);
% Cut first 10 datapoints of the first derivative
vector to prevent too early endpoint detection
    X = zeros(1,length(derivative4));
% Create vector X with zeros
    for i = 1:length(derivative4)-1
% Find point: negative to positive derivative, give
this point value 100 in X vector
        if derivative4(i) < 0 && derivative4(i+1) > 0
        X(i) = 100;
        XX = find(X==100);
        MitoVO2_end = XX+10;
        end
    end
    end
end


% If the dynamic mitoPO2 measurement did not contain
an ascending part, mitoVO2_end is manually determined
MitoVO2_end = length(MitoPO2);
OR
MitoVO2_end = locs1(1);

% Endpoint of the descending part of the optimized
fitted curve
t_VO2_end = t(MitoVO2_end);
```

Starting point of the descending part of the optimized fitted curve = MitoVO2_start

```
% If the first point of the derivative is < -0.25,
MitoVO2_start = 1
if derivative3(1) < -0.25
    MitoVO2_start = 1;
End

k = 1;
%If the first point of the derivative is > -0.25
if derivative3(1) > -0.25
    k2_VO2 = k2(1:MitoVO2_end);
% Select baseline + descending part
    [pks_des, locs_des] = findpeaks(k2_VO2);
% Findpeaks
    del_des = find(pks_des<0);
% Delete negative peaks
    pks_des(del_des) = [];
    locs_des(del_des) = [];
    sorted_VO2 = sort([pks_des, locs_des], 'descend');
% Sortpeaks
    sorted_locs_VO2 = sorted_VO2(:,1);
% Locations of the peaks
    sorted_pks_VO2 = sorted_VO2(:,2);
% Peak heights
    MitoVO2_start = sorted_locs_VO2(k);
% MitoVO2_start = peak at location k = 1 / 2 / 3 ...

% However, if the peak at k = @@ is wide and < 0.015 /
< 0.02 in height, select k + 1/2 as MitoVO2_start
    point = MitoVO2_start;
    if (k2(point)-k2(point+1)) < 0.015
        MitoVO2_start = point+1;
    end
    if (k2(point)-k2(point+2)) < 0.02
        MitoVO2_start = point+2;
    end
end

% Starting point of the descending part of the
optimized fitted curve
t_VO2_start = t(MitoVO2_start);
```

```
% Plot starting point and endpoint of the descending
part of the optimized fitted curve
figure(7)
hold on
plot(t,MitoPO2);
plot(t,a);
plot(t_VO2_start,a(MitoVO2_start), '*');
plot(t_VO2_end,a(MitoVO2_end), '*');
legend('Raw mitoPO2 signal', 'Optimized fitted curve')
xlabel('Time (s)','FontSize',16);
ylabel('MitoPO2 (mm Hg)','FontSize',16);
```

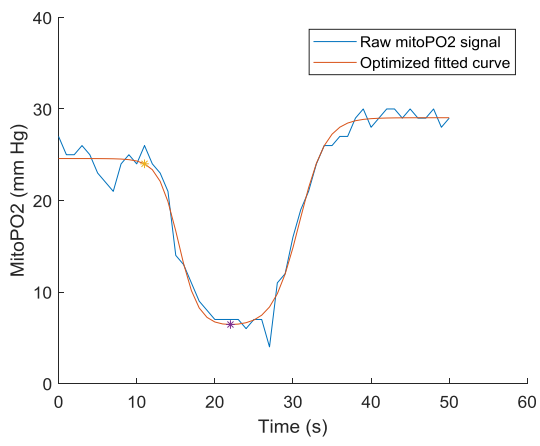

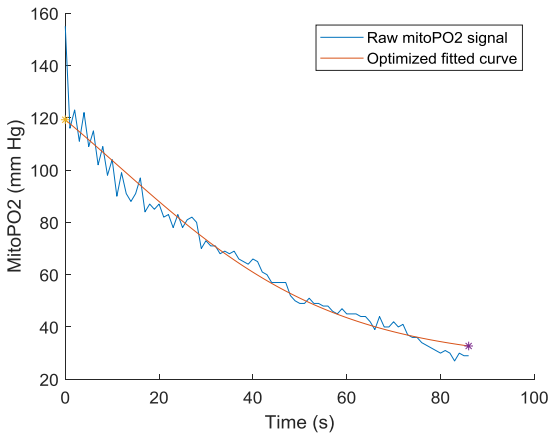

Step 8: Calculate mitoPO$_{2_baseline}$, mitoVO$_{2_max}$ and root mean squared error (RMSE) of the descending part of the optimized fitted curve

MitoPO$_{2_baseline}$ was determined by averaging the first three mitoPO$_2$ samples of the dynamic mitoPO$_2$ measurement. However, if the variance between these three mitopO$_2$ samples was greater than 20, it was assumed that the mitoPO$_2$ directly descends at the beginning of the dynamic mitoPO$_2$ measurement. In that case, the first mitoPO$_2$ sample was selected as mitoPO$_{2_baseline}$. MitoVO2$_{_max}$ was determined via the minimum value of the first derivative of the optimized fitted curve.

```
% MitoVO2_max = the minimum of the first derivative of
the optimized fitted curve
[MitoVO2_max, ind_MitoVO2_max] = min(derivative3);
MitoVO2_max = -1*MitoVO2_max;
% Index MitoVO2_max
ind_MitoVO2_max = ind_MitoVO2_max + 1;

% Root mean squared error calculated by the formula:
sqrt(sum((fit-data).^2)/length(data))
[error_descending_part] =
errorfunction(MitoPO2(MitoVO2_start:MitoVO2_end),a(Mit
oVO2_start:MitoVO2_end));

% MitoPO2_baseline
% Create empty vector
o = [];
% Look at samples 1 t/m 10
for i = 1:10
% If SNR of sample i is >=5
    if SNR(i) >=5
% Add MitoPO2(i) to empty vector. Vector o is filled
with MitoPO2 samples with an  >=5
        o = [o MitoPO2(i)];
    end
end

% Calculate variance of the first three mitoPO2
samples of vector o
variance = var(o(1:3));
% If variance > 20, mitoPO2_baseline is the first
MitoPO2 sample of vector o
if variance > 20

        MitoPO2_baseline = o(1);
end

% If variance < 20, mitoPO2_baseline is the mean of
the first three mitoPO2 samples of vector o
if variance < 20

    MitoPO2_baseline = mean(o(1:3));
End
```

Step 9: Plot final figure

```
figure(8);
hold on;
plot(t,MitoPO2);
plot(t,a);
plot(t_VO2_start,a(MitoVO2_start), '*');
plot(t_VO2_end,a(MitoVO2_end), '*');
plot(t(ind_MitoVO2_max), a(ind_MitoVO2_max), '*');

a = gca;
a.Position(3) = 0.6;
annotation('textbox', [0.70, 0.15, 0.1, 0.1],
'String', "RMSE = " + num2str(error_descending_part))
annotation('textbox', [0.70, 0.25, 0.1, 0.1],
'String', "MitoPO2 baseline = " +
num2str(MitoPO2_baseline))
annotation('textbox', [0.70, 0.35, 0.1, 0.1],
'String', "MitoVO2 max = " + num2str(MitoVO2_max))
xlabel('Time (s)','FontSize',14);
ylabel('MitoPO2 (mmHg)','FontSize',14);

legend('Raw mitoPO2 signal', 'Optimized fitted curve')
xlabel('Time (s)','FontSize',16);
ylabel('MitoPO2 (mm Hg)','FontSize',16);
ax = gca;
ax.FontSize = 12;
```

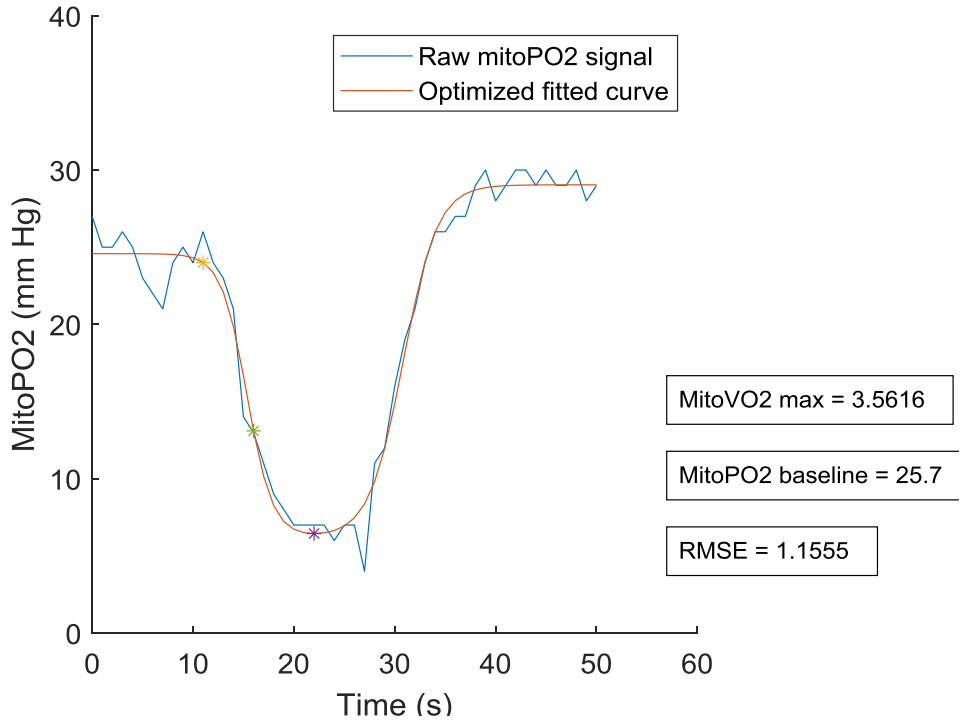

Background information about the curvature formula

The curvature at a point *M* of a curve is defined as:

$$k = \frac{d\alpha}{ds}$$

where α is the angle of the inclination of the tangent line with M, as shown in the figure below. Thus the curvature is the absolute value of the rate change of α with respect to the arc length *s*. The curvature (*k*) can be regarded as a measure of change of the direction of the curve.

$$k = \frac{d\alpha}{ds} = \frac{d\alpha}{dx} * \frac{dx}{ds}$$

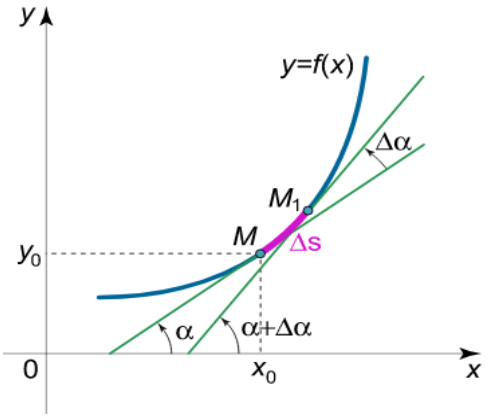

Part 1: derive $d\alpha/dx$

Tangent of α (tan α) is the opposite over adjacent:

$$\tan\alpha = \frac{dy}{dx}$$

$$\alpha = \arctan\left(\frac{dy}{dx}\right)$$

Formula for differentiating the arctan is:

$$\frac{d(\arctan u)}{dx} = \frac{\frac{du}{dx}}{1+u^2}$$

Substitute dy/dx wherever there is an **u**:

$$\frac{d\alpha}{dx} = \frac{d\left(\arctan\left(\frac{dy}{dx}\right)\right)}{dx} = \frac{d\left(\frac{dy}{dx}\right)}{1+\left(\frac{dy}{dx}\right)^2} = \frac{\frac{d^2y}{dx^2}}{1+\left(\frac{dy}{dx}\right)^2}$$

Part 2: Derive dx/ds

$$\frac{dx}{ds} = \frac{1}{\frac{ds}{dx}}$$

Using the Pythagorean Theorem:

$$ds = \sqrt{dx^2 + dy^2}$$

Square both sides:

$$ds^2 = dx^2 + dy^2$$

Divide every term by dx^2:

$$\frac{ds^2}{dx^2} = \frac{dx^2}{dx^2} + \frac{dy^2}{dx^2}$$

Square root both sides:

$$\frac{ds}{dx} = \sqrt{1 + \left(\frac{dy}{dx}\right)^2}$$

$$\frac{dx}{ds} = \frac{1}{\sqrt{1 + \left(\frac{dy}{dx}\right)^2}}$$

CURVATURE FORMULA:

$$k = \frac{d\alpha}{ds} = \frac{d\alpha}{dx} * \frac{dx}{ds} = \frac{\frac{d^2y}{dx^2}}{1 + \left(\frac{dy}{dx}\right)^2} * \frac{1}{\sqrt{1 + \left(\frac{dy}{dx}\right)^2}} = \frac{\frac{d^2y}{dx^2}}{\left(1 + \left(\frac{dy}{dx}\right)^2\right)^{\frac{3}{2}}} = \frac{f''(x)}{(1 + (f'(x)^2)^{\frac{3}{2}}}$$

APPENDIX II

Interim analysis: three analysis methods to derive a measure for mitochondrial oxygen consumption

In recent years, several methods have been published to derive a measure for mitochondrial oxygen consumption ($mitoVO_2$) from a dynamic mitochondrial oxygen tension ($mitoPO_2$) measurement.

Michaelis-Menten method

Harms et. al. used the Michaelis-Menten kinetics to calculate the oxygen disappearance rate (ODR) (1). The principle of ODR measurements is shown in **Figure 1**.

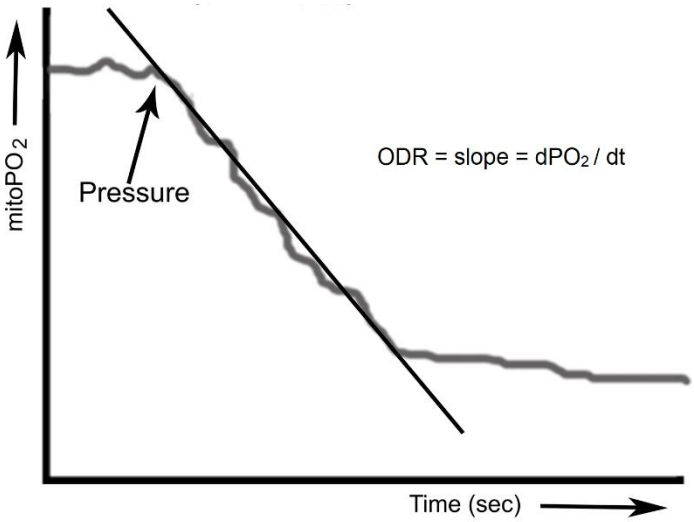

Figure 1: Principle of mitochondrial oxygen consumption ($mitoVO_2$) by pressure-induced occlusion of the microcirculatory blood flow. $MitoVO_2$ is calculated from the linear part of the oxygen disappearance curve. Printed from: Harms et.al. (1)

The mitochondrial oxygen tension ($mitoPO_2$) inside the measurement volume reflects the balance between oxygen consumption inside the measurement volume and oxygen inflow into the measurement volume. The total oxygen consumption consists of $mitoVO_2$ and the additional oxygen consumption induced by the measurement procedure. Oxygen consumption by the measurement procedure is caused by photo consumption (2). Due to photo consumption, each excitation pulse with green light consumes a small part of the oxygen that is present in the mitochondria. This can result in an overestimation of the $mitoVO_2$ (3). However, Harms et.al. measured no oxygen disappearance due to photo consumption at relatively high $mitoPO_2$ levels induced by the blockade of oxygen consumption by cyanide (1). This result indicates that ODR could be analyzed without taking oxygen consumption by the measurement procedure into account.

Applying pressure on the measurement volume with the measurement probe of the COMET monitor creates a no-flow condition. During this condition, microcirculatory oxygen supply is stopped and $mitoPO_2$ inside the measurement volume will drop due to oxygen consumption by the mitochondria. The difference in PO_2 between the measurement volume and the surrounding tissue gradually increases during the no-flow condition and therefore oxygen starts to diffuse into the measurement volume. The rate of oxygen disappearance within the measurement volume during the no-flow condition is described by the following formula:

$$(1)\quad \mathrm{ODR} = \frac{\mathrm{dmitoPO2(t)}}{\mathrm{dt}} = \mathrm{-mitoVO2(t)\text{-}OCM(t) + DOI(t)}$$

where $dPO_2(t)/dt$ is the ODR at time point t, $mitoVO_2(t)$ is the mitochondrial oxygen consumption, *OCM(t)* is the Oxygen Consumption by the Measurement procedure and *DOI(t)* is the Diffusive Oxygen Influx into the measurement volume.

The idea behind the Michaelis-Menten kinetics is that the disappearance of mitoPO$_2$ after occlusion of the microcirculatory blood flow behaves like an enzyme reaction, which converts substrate molecules to products. This enzyme reaction depends on some intrinsic characteristics, namely the not supply-dependent maximal mitochondrial oxygen consumption (*Vmax*) and the mitoPO$_2$ at which mitochondrial oxygen consumption is reduced to ½*Vmax (*P50*). The reaction rate also depends on the concentration of the substrate, the amount of oxygen that is still left in the mitochondrial measurement volume at time point t (mito*PO$_2$(t)*).

When translating this to a dynamic mitoPO$_2$ measurement, mitoVO$_2$(t) can be described by the following formula according to the Michaelis-Menten kinetics:

$$(2) \quad \text{mitoVO2(t)} = \frac{\text{Vmax*mitoPO2(t)}}{\text{P50} + \text{mitoPO2(t)}}$$

where *Vmax* is the not supply-dependent maximal tissue oxygen consumption, *P50* is the mitoPO$_2$ at which mitochondrial oxygen consumption is reduced to ½**Vmax* and *mitoPO$_2$(t)* is the mitoPO$_2$ in the measurement volume at time point t.

When combining equations 1 and 2, not taking *OCM(t)* into account, this results in the following differential equation:

$$\text{ODR} = \frac{\text{dmitoPO2(t)}}{\text{dt}} = \frac{\text{Vmax*mitoPO2(t)}}{\text{P50} + \text{mitoPO2(t)}} + \text{DOI (t)}$$

For a good fit using the Michaelis-Menten method, three parameters need to be estimated from a dynamic mitoPO$_2$ measurement, namely Vmax, P50 and initial mitoPO$_2$. From this Michaelis-Menten fit, maximum oxygen consumption (mitoVO$_{2_max}$) can be derived as mitoVO$_2$ measure by taking the minimum value of the first derivative of the Michaelis-Menten fit.

Sigmoid function method

A research group from Germany used a sigmoid function to fit the descending part of the raw mitoPO$_2$ signal (4):

$$\frac{\text{dmitoPO2(t)}}{\text{dt}} = \frac{\text{K1}}{1 + e^{(\text{-B1*(x-M1)})}} + \text{Z}$$

K1 is the baseline mitoPO$_2$ level before inhibition of the microcirculation, *B1* modulates the slope for oxygen consumption, *M1* indicates the time of maximum oxygen consumption during inhibition of the microcirculation and *Z* is the minimum mitoPO$_2$ level after inhibition of the microcirculation. To fit this sigmoid function on the raw mitoPO$_2$ signal, these four parameters need to be estimated. From this sigmoid fit, mitoVO$_{2_max}$ can be derived as mitoVO$_2$ measure by taking the minimum value of the first derivative of the Sigmoid function fit.

Linear estimation method

The third method is a self-developed linear estimation method. This method smooths the raw mitoPO$_2$ signal by using a moving average filter. A moving average filter returns a moving average of the mitoPO$_2$ samples of the dynamic mitoPO$_2$ measurement using a fixed window length. This window slices down the length of the raw mitoPO$_2$ signal, computing an average over the mitoPO$_2$ samples within each window. MitoVO$_{2_max}$ can be derived by taking the minimum value of the first derivative of this smoothed mitoPO$_2$ signal. Hence, no parameters need to be estimated because mitoVO$_{2_max}$ is directly retrieved from the data.

Small study

During an interim analysis, both the Michaelis-Menten method, the sigmoid function method and the linear estimation method were compared by evaluating their performance on multiple dynamic mitoPO$_2$ measurements of twelve critically ill septic patients admitted to the Intensive Care Unit of the Leiden University Medical Centre. First of all, several dynamic mitoPO$_2$ measurements were excluded for further analysis due to poor signal quality or due to non-inducible mitoVO$_2$ (no decrease in mitoPO$_2$ after applying pressure). For each dynamic mitoPO$_2$ measurement, mitoVO$_{2_max}$ and root mean square error (RMSE) were calculated. The RMSE provides information about the performance of the fit. The RMSE is defined as the sum of the square of the error between raw mitoPO$_2$ signal (data) and the fit:

$$\mathrm{RMSE} = \frac{\sqrt{\sum_t^{tend}(\text{fit-data})^2}}{N}$$

where *N* is the number of mitoPO$_2$ samples.

A lower RMSE between the raw mitoPO$_2$ signal and the fit indicates a better fit performance. Two examples of dynamic mitoPO$_2$ measurements with the different fit methods and derived mitoVO$_{2_max}$ and RMSE values are shown in **Figure 2**.

Advantages and disadvantages of each method

*Michaelis-Menten method (Michaelis_Menten.*m)*

- ⊕ Compared to the linear estimation method, the Michaelis-Menten method is less sensitive for outliers when deriving mitoVO$_{2_max}$.

- ⊗ In general, mitoVO$_{2_max}$ is underestimated by the Michaelis-Method method. Michaelis-Menten kinetics assumes that mitoVO$_2$ is oxygen-dependent. According to Michaelis-Menten kinetics, the mitoPO$_2$ descends steeply at the beginning of the oxygen consumption phase because of the high oxygen concentration in the mitochondria (**Figure 2A**). However, most dynamic mitoPO$_2$ measurements showed a slow increase in descending rate at the beginning of the oxygen consumption phase (**Figure 2B**). This behaviour is not in line with the Michaelis-Menten kinetics and therefore, the Michaelis-Menten fit did not follow the steepest part of the raw mitoPO$_2$ signal (**Figure 2B**). This is the reason that the Michaelis-Menten method showed higher RMSE values for most of the dynamic mitoPO$_2$ measurements.
- ⊗ Since three parameters need to be estimated, fit performance gets worse when less mitoPO$_2$ samples are measured during the dynamic mitoPO$_2$ measurements.

*Sigmoid function method (Sigmoid.*m)*

- ⊕ Compared with the linear method, the sigmoid method is less sensitive for outliers when deriving mitoVO$_{2_max}$.
- ⊕ Compared to the Michaelis-Menten method, the sigmoid method showed lower RMSE values. In general, the sigmoid method seems to have a fit good performance on several types of data curves (**Figure 2C, 2D**), whereas the Michaelis-Menten method has only a good fit on dynamic mitoPO$_2$ measurements that matches the Michaelis-Menten kinetics (**Figure 2A, 2B**).
- ⊕ A second sigmoid function can be added to the existing sigmoid function to create two complementary sigmoid functions. This second sigmoid function is able to fit the ascending part of the raw mitoPO$_2$ signal and can be used to derive a measure for mitochondrial oxygen delivery (mitoDO$_2$). MitoDO$_2$ is a newly introduced parameter for mitochondrial reoxygenation (4). This newly introduced parameter for mitochondrial reoxygenation might be an indirect parameter of the microcirculatory function because mitochondrial reoxygenation is dependent on the microcirculatory oxygen supply.

$$\frac{K1}{1 + e^{(-B1*(x-M1))}} + \frac{K2}{1 + e^{(-B2*(x-M2))}} + Z$$

K1 = baseline mitoPO2 level before inhibition of the microcirculation
K2 = mitoPO2 level after reoxygenation
B1 = slope modulation for oxygen consumption
B2 = slope modulation for reoxygenation
M1 = time of maximum oxygen consumption during inhibition of the microcirculation
M2 = time of maximum reoxygenation after pressure release
Z = minimum mitoPO2 level after inhibition of the microcirculation

⊗ Since four parameters need to be estimated, fit performance gets worse when less mitoPO2 samples are measured during the dynamic mitoPO2 measurements.

*Linear estimation method (Linear.*m)*

⊕ Since no parameter has to be estimated, the linear estimation method has the highest fit performance. This is the reason that the linear estimation method showed the lowest RMSE values for all the dynamic mitoPO2 measurements (**Figure 2E, 2F**).

⊗ The linear method is very sensitive for outliers when deriving a measure for mitoVO2_max.
⊗ Physiologically, it is not expected that mitochondrial oxygen consumption is linear during the whole oxygen consumption phase.

2A

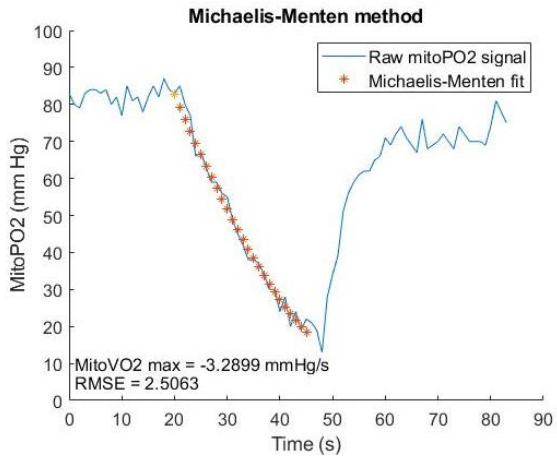

2B

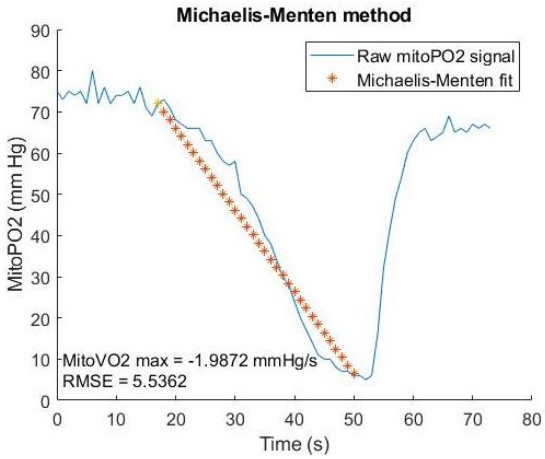

2C

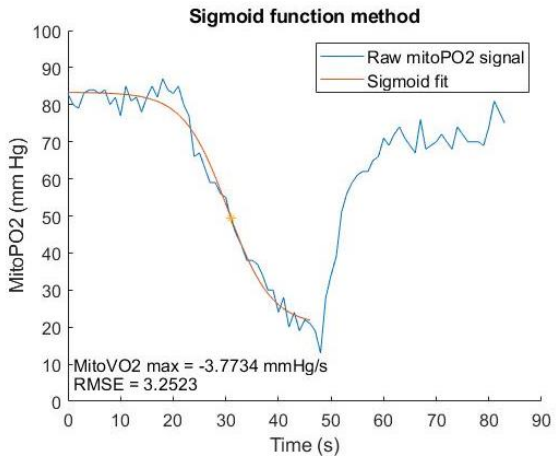

2D

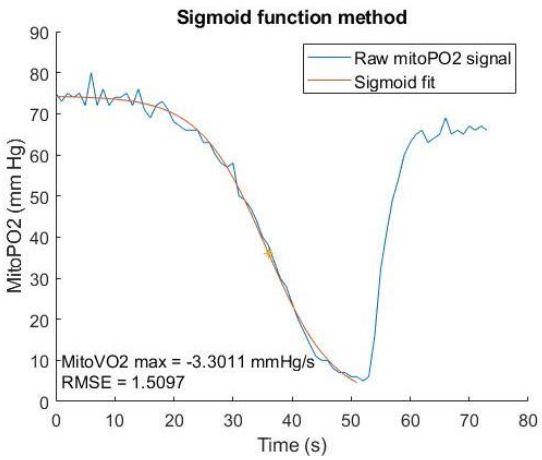

2E

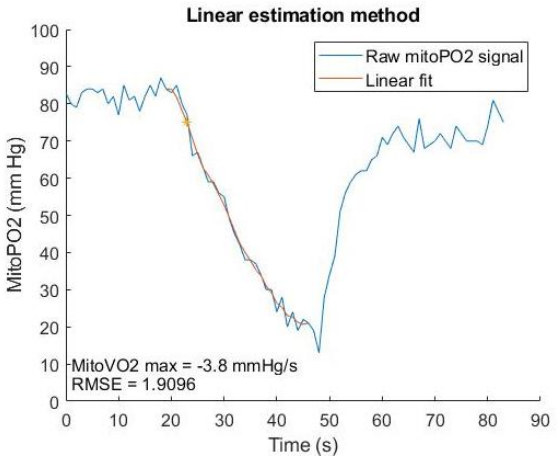

2F

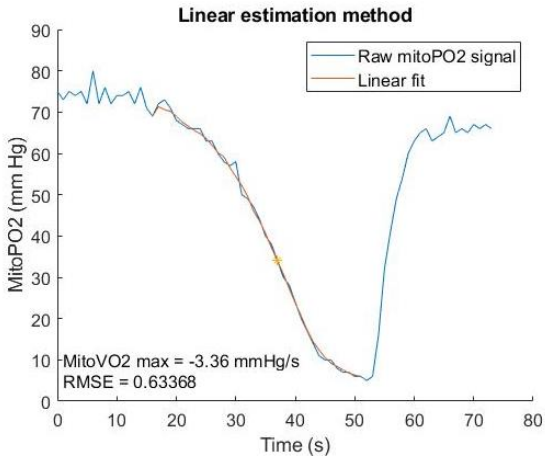

Figure 2 : Two examples of dynamic mitochondrial oxygen tension ($mitoPO_2$) measurements with the three different fitting methods and the derived maximum oxygen consumption ($mitoVO_{2\_max}$) and root mean squared error (RMSE) values.

Conclusion

During this interim analysis, three data analysis methods were developed in MATLAB to derive a measure for mitoVO$_2$ from dynamic mitoPO$_2$ measurements. Michaelis-Menten kinetics assumes that mitochondrial oxygen consumption is oxygen-dependent. However, most dynamic mitoPO$_2$ measurements showed a slow increase in descending rate at the beginning of the oxygen consumption phase. This behaviour is not in line with the Michaelis-Menten kinetics. Whereas the Michaelis-Menten method has only a good fit performance on dynamic mitoPO$_2$ measurement that matches the Michaelis-Menten kinetics, the sigmoid function method has a good fit performance on several types of data curves. Furthermore, the sigmoid function method is less sensitive for outliers compared to the linear estimation method. These are the two main reasons that we chose for the sigmoid function method as the final analysis method for the study.

References

1. Harms FA, Voorbeijtel WJ, Bodmer SI, Raat NJ, Mik EG. Cutaneous respirometry by dynamic measurement of mitochondrial oxygen tension for monitoring mitochondrial function in vivo. Mitochondrion. 2013;13(5):507-14.
2. Mitra S, Foster TH. Photochemical oxygen consumption sensitized by a porphyrin phosphorescent probe in two model systems. Biophys J. 2000;78(5):2597-605.
3. Golub AS, Tevald MA, Pittman RN. Phosphorescence quenching microrespirometry of skeletal muscle in situ. Am J Physiol Heart Circ Physiol. 2011;300(1):H135-43.
4. Baumbach P, Neu C, Derlien S, Bauer M, Nisser M, Buder A, et al. A pilot study of exercise-induced changes in mitochondrial oxygen metabolism measured by a cellular oxygen metabolism monitor (PICOMET). Biochim Biophys Acta Mol Basis Dis. 2019;1865(4):749-58.

APPENDIX III

Association between mitochondrial oxygenation and oxygen consumption

The Cellular Oxygen METabolism (COMET) monitor measures mitochondrial oxygen tension (mitoPO$_2$) with delayed fluorescence of mitochondrial protoporphyrin IX (PpIX) (1-2). MitoPO$_2$ is the resultant of mitochondrial oxygen supply and the amount of oxygen consumed by the mitochondria. Blocking microcirculatory blood flow by pressing the measurement probe on the skin allows the measurement of mitochondrial oxygen consumption (mitoVO$_2$) (3). This procedure induced measurable oxygen consumption rates due to cessation of the microcirculatory oxygen supply and ongoing oxygen consumption by the mitochondria. In this study, mitoPO$_2$ was measured before (static) and during the application of pressure (dynamic). The mitoPO$_2$ measured at baseline level was defined as mitoPO$_{2_baseline}$. The maximum rate of mitoPO$_2$ change during the stop-flow condition was defined as mitoVO$_{2_max}$. We investigated the association between the static mitochondrial parameter (i.e. mitoPO$_{2_baseline}$) and the dynamic mitochondrial parameter (i.e. mitoVO$_{2_max}$). We divided mitoPO$_{2_baseline}$ into three groups: low, medium and high for this longitudinal analysis (**Figure 1A**). Just like mitoPO$_{2_baseline}$, mitoVO$_{2_max}$ can also be divided into three groups (fast, medium, slow) to better understand the interaction between mitoPO$_{2_baseline}$ and mitoVO$_{2_max}$ (**Figure 1B**).

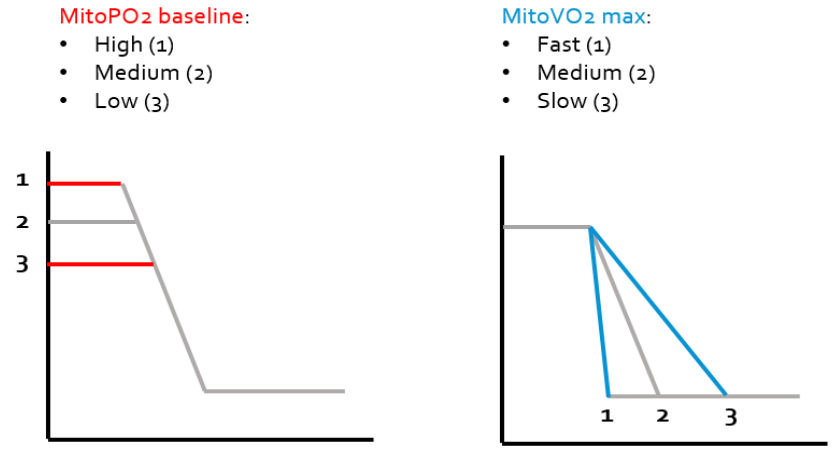

Figure 1A **Figure 1B**

Figure 1A: The three mitoPO$_{2_baseline}$ groups: high(1), medium(2), low(3).
Figure 1B: The three mitoVO$_{2_max}$ groups: fast(1), medium(2), slow(3).
Medium levels (gray) are the reference levels.

Hypothesis

As stated above, mitoPO$_2$ is a resultant of mitochondrial oxygen supply and consumption (**Figure 2**).

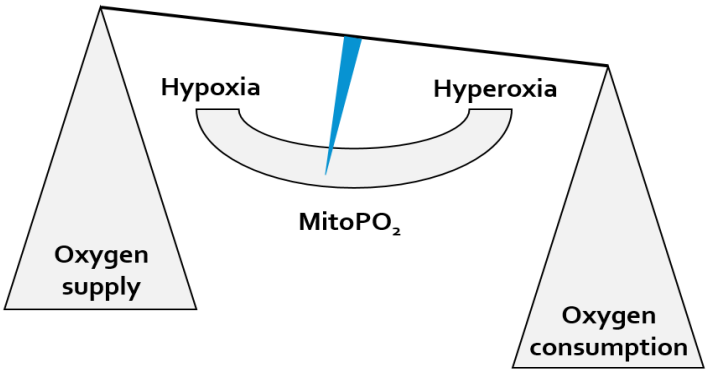

Figure 2: The oxygen balance. Mitochondrial oxygen tension (mitoPO$_2$) is the resultant of mitochondrial oxygen supply and consumption.

Mitochondria with medium and high $mitoPO_{2\_balance}$ levels, the 'happy mitochondria', have a stable balance between oxygen supply and consumption. This balance will be shifted to more oxygen consumption and less oxygen supply in mitochondria with low $mitoPO_{2\_baseline}$ levels, the 'unhappy' mitochondria.

We hypothesize that the rate of $mitoPO_2$ change during the temporary cessation of the microcirculatory blood flow provides us information about how quickly the mitochondria suffer from the acute cessation of the oxygen supply. The rate of $mitoPO_2$ change indicates how fast the mitochondria consume the present oxygen.

We will describe our hypothesis by four different situations:

- High $mitoPO_{2\_baseline}$ (1) and low $mitoVO_{2\_max}$ (3) (**Figure 3A**):
    - These mitochondria won't be directly affected by the acute cessation of the microcirculatory oxygen supply because of their oxygen reserves > slow oxygen consumption > slow decline in $mitoPO_2$.
- High $mitoPO_{2\_baseline}$ (1) and fast $mitoVO_{2\_max}$ (1) (**Figure 3B**):
    - These mitochondria will be directly affected by the acute cessation of the microcirculatory oxygen supply > rapid oxygen consumption > rapid decline in $mitoPO_2$.
- Low $mitoPO_{2\_baseline}$ (1) and low $mitoVO_{2\_max}$ (1) (**Figure 3C**):
    - These mitochondria are not directly affected by the acute cessation of the microcirculatory oxygen supply because these mitochondria will partially shutdown and will reduce their oxygen consumption > slow oxygen consumption > slow decline in $mitoPO_2$.
- Low $mitoPO_{2\_baseline}$ (1) and high $mitoVO_{2\_max}$ (1) (**Figure 3D**):
    - The $mitoPO_{2\_baseline}$ is unfavorable. These mitochondria are most likely 'unhappy' and in stress. These mitochondria will be directly affected by the acute cessation of the microcirculatory oxygen supply. The oxygen balance will be shifted to more oxygen consumption (**Figure 2**) > rapid oxygen consumption > rapid decline in $mitoPO_2$.

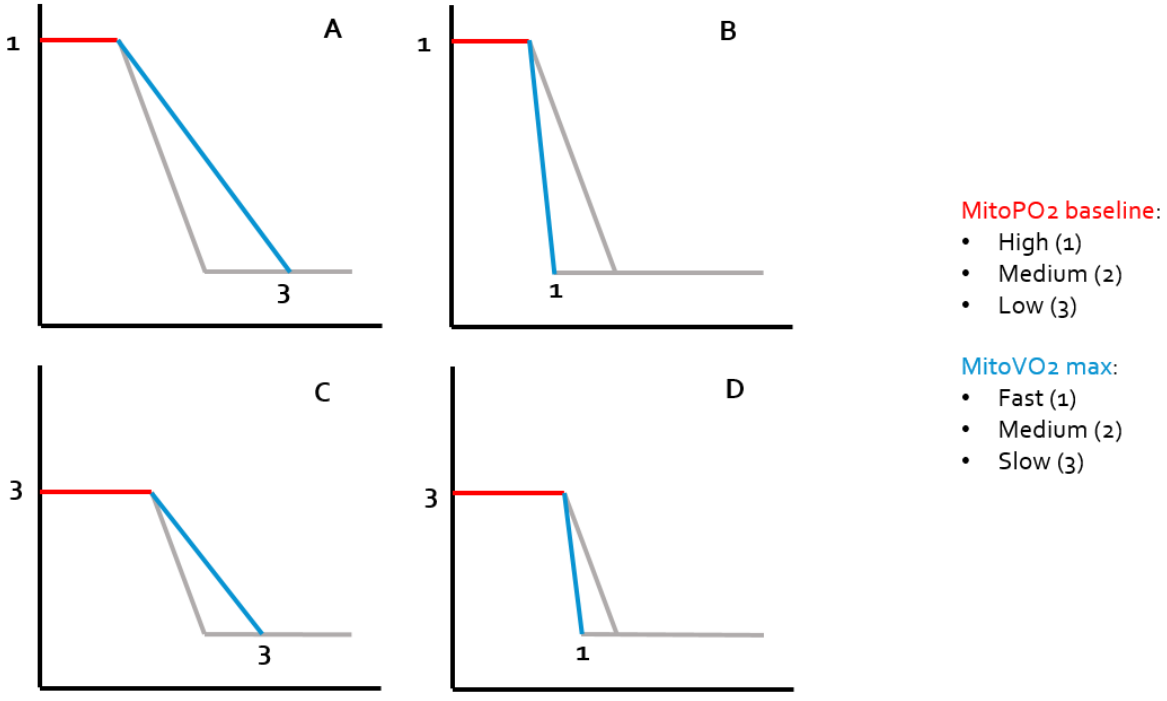

Figure 3: The four different situations.
Figure 3A: High baseline mitochondrial oxygen tension ($mitoPO_{2\_baseline}$) and slow maximum mitochondrial oxygen consumption ($mitoVO_{2\_max}$).
Figure 3B: High $mitoPO_{2\_baseline}$ and fast $mitoVO_{2\_max}$.
Figure 3C: Low $mitoPO_{2\_baseline}$ and slow $mitoVO_{2\_max}$.
Figure 3D: Low $mitoPO_{2\_baseline}$ and fast $mitoVO_{2\_max}$.
Medium levels (gray) are the reference levels.

References

1. Mik EG, Stap J, Sinaasappel M, Beek JF, Aten JA, van Leeuwen TG, et al. Mitochondrial PO2 measured by delayed fluorescence of endogenous protoporphyrin IX. Nat Methods. 2006;3(11):939-45.
2. Ubbink R, Bettink MAW, Janse R, Harms FA, Johannes T, Munker FM, et al. A monitor for Cellular Oxygen METabolism (COMET): monitoring tissue oxygenation at the mitochondrial level. J Clin Monit Comput. 2017;31(6):1143-50.
3. Harms FA, Voorbeijtel WJ, Bodmer SI, Raat NJ, Mik EG. Cutaneous respirometry by dynamic measurement of mitochondrial oxygen tension for monitoring mitochondrial function in vivo. Mitochondrion. 2013;13(5):507-14.

APPENDIX IV

Database

Patient	Gender[1]	Age	Source[2]	APACHE	Time[3]	MitoPO2 baseline	MitoPO2 baseline group[4]	MitoVO2 max[5]	RMSE	Lactate	ScvO2
1	1	63	1	36	0	53	2	2,34	1,33	1,5	
1	1	63	1	36	2	35,3	1	3,66	0,91	1,4	
1	1	63	1	36	4	78,3	3	5,69	2,57	1,6	
2	1	72	2	85	0	63	3	2,87	1,59	2,2	
2	1	72	2	85	2	63,7	3	1,28	1,52	2,1	
2	1	72	2	85	14	155	3	1,59	5,35	1,7	
3	1	68	3	118	0	51	2	0,2	2,62	9,3	91
3	1	68	3	118	2	40,7	2	3,09	1,61	10	88
3	1	68	3	118	4	49	2	3,47	1,79	8,8	84
3	1	68	3	118	6	3,3	1	0		10,4	74
3	1	68	3	118	20	26,7	1	3,61	1,47	6,9	
4	2	34	4	22	0	67	3	3,5	2,01	0,9	
4	2	34	4	22	2	63	3	3,96	1,51	0,8	
4	2	34	4	22	4	40,3	2	2,05	1,17	0,8	
4	2	34	4	22	6	98	3	2,35	0,9	1	
4	2	34	4	22	20	80,3	3	2,61	2,64		
6	2	58	2	93	0	55	2	0		1,4	
6	2	58	2	93	2	57,7	2	0,29	1,91	1,5	
6	2	58	2	93	4	74,3	3	3,37	1,39	1,5	
6	2	58	2	93	6	46,7	2	2,72	1,66	1,8	
6	2	58	2	93	8	81,7	3	1,52	3,63	1,5	
6	2	58	2	93	19	80,7	3	3,66	3,43	1,1	
7	1	71	5	62	0	59	2	2,56	1,61	1	
7	1	71	5	62	2	76,7	3	1,84	1,87	0,8	
7	1	71	5	62	13	67,7	3	2,78	5,63	1,9	
8	2	67	5	65	0	59	2	1,91	0,87	2,6	
8	2	67	5	65	2	63,7	3	2,15	1,93	2,5	80
8	2	67	5	65	4	76,3	3	2,48	1,25	2,8	78
8	2	67	5	65	6	81	3	2,63	2	3,1	74
9	1	82	5	46	0	71,7	3	2,43	3,63	1	69
9	1	82	5	46	13	112,3	3	4,09	4,53	1	69
10	1	54	5	42	0	187	3	-		0,7	
10	1	54	5	42	2	76	3	2,1	1,67	0,6	
10	1	54	5	42	4	13,3	1	0		0,6	
10	1	54	5	42	8	12,3	1	0		0,7	
11	1	60	3	47	0	47	2			2,2	82
11	1	60	3	47	13	82	3	-		1,5	81
11	1	60	3	47	15	43	2			2,1	75
11	1	60	3	47	17	62,3	3	6,33	2,08	2,1	69
11	1	60	3	47	19	39,7	1	8,82	1,55	2,3	74
11	1	60	3	47	21	62	2	9,18	1,58	1,4	79
12	1	69	5	87	0	62,3	3	3,63	2,03	2,6	
12	1	69	5	87	13	71,3	3	1,82	2,57	1,6	83
12	1	69	5	87	15	68	3	3,35	3,56	1	85

12	1	69	5	87	17	69,7	3	4,54	2,29	1,4	86
12	1	69	5	87	19	62	2	-		1,6	89
13	1	61	2	84	0	54,3	2			2,2	
13	1	61	2	84	2	45,7	2			3	
13	1	61	2	84	5	41,7	2	3,87	1,2	2,9	
13	1	61	2	84	7	44	2	4,31	1	2,4	
13	1	61	2	84	9	19,3	1	1,8	0,8	2	
13	1	61	2	84	20	29	1	3,45	1,18		
14	2	46	4	62	0	101	3	0		3,7	57
14	2	46	4	62	2	96	3	0		2,8	42
14	2	46	4	62	5	99	3	2,53	3,24	2,3	48
14	2	46	4	62	7	78	3	1,55	4,57	1,8	68
14	2	46	4	62	9	141	3			1,6	61
14	2	46	4	62	21						
15	1	62	3	103	0	51	2	0		2,7	
15	1	62	3	103	3	47,7	2	0		2,3	85
15	1	62	3	103	5	47	2	-		2,8	82
15	1	62	3	103	7	57	2	2,02	2,36	2,6	81
15	1	62	3	103	9	38,7	1	1,63	1,52	2,8	80
15	1	62	3	103	11	61,3	2	2,02	1,54	2,8	80
15	1	62	3	103	22	19	1	2,34	0,9	2,8	83
16	1	67	3	70	0	41	2	9,23	1,31	5,5	
17	1	69	3	114	0	59,7	2	8,62	1,66	1,7	82
17	1	69	3	114	3	54,3	2	7,3	2,5	1,6	86
17	1	69	3	114	5	25,7	1	3,56	1,16	2	88
17	1	69	3	114	7	11,3	1	0,78	1,4	1,2	86
17	1	69	3	114	9	1,7	1	0		1,3	85
17	1	69	3	114	11	2,7	1	0		1,2	87
18	1	66	3	114	0	35,3	1	0		1,2	
18	1	66	3	114	2					1,3	
18	1	66	3	114	4	15,7	1	0		1	
18	1	66	3	114	6	75	3	1,13	5,36	1,1	
18	1	66	3	114	8	59,3	2	1,53	2,51	1,3	
18	1	66	3	114	10	37,3	1	0,44	2,25	1,4	
18	1	66	3	114	12	6,3	1	0		1,2	
19	2	70	3	93	0	53	2	-		1,2	
19	2	70	3	93	10	91	3	2,65	3,77	1,2	
19	2	70	3	93	14	92	3	2,23	3,3	1,2	
19	2	70	3	93	17	45,7	2	1,86	2,61	1,1	66
19	2	70	3	93	20	61	2	3,21	2,39	1,2	70
20	2	66	3	75	0	27,3	1	3,76	2,01	1,9	
20	2	66	3	75	2	45	2			1,9	
20	2	66	3	75	3	13,3	1	5,47	0,83	1,6	
20	2	66	3	75	5	7	1	0,28	1,58	1,5	
21	1	42	5	51	0	79,7	3	1,38	4,29	2	

21	1	42	5	51	5	61,7	2	5,22	1,13	2,1	
21	1	42	5	51	6	48	2	3,98	2,11	2,1	
21	1	42	5	51	8	50	2	0,81	1,93	1,7	
22	1	52	6	93	0	41	2	6,35	2,95	3,9	
22	1	52	6	93	3	18,3	1	9,9	1,85	4,2	71
22	1	52	6	93	6	20,7	1	11,75	1,53	3,2	70
22	1	52	6	93	8	31	1	5,96	0,96	3,2	72
22	1	52	6	93	20	69,3	3	5,96	2,24	2,9	
26	1	82	5	74	0	117	3	3,23	5,65	1,2	
26	1	82	5	74	3	85	3	3,23	1,55		
26	1	82	5	74	4	73	3	5,19	2,7	1,4	
26	1	82	5	74	6	70	3	2,93	2,77	1,3	
26	1	82	5	74	20	102	3	5,99	5,59		
27	2	73	5	57	0	32,3	1	4,24	0,96		
27	2	73	5	57	2	96	3	4,49	4,44	2	
27	2	73	5	57	4	56	2	2,02	3,05	2	
27	2	73	5	57	5	123	3	2,89	6,32	2,1	
27	2	73	5	57	8	82,3	3	4,31	2,09	2	
27	2	73	5	57	10	34	1	3,73	1,68	1,8	
28	1	52	4	45	0	64,7	3			0,7	
28	1	52	4	45	1	48,3	2	4,24	1,96	0,5	
29	1	50	4	52	0	55	2	3,21	2,34	2,4	
29	1	50	4	52	3	23,7	1	2,97	0,86	2,9	
29	1	50	4	52	5	103	3	0,73	3,63	1,8	
29	1	50	4	52	16	10,3	1	0,42	0,77		
30	1	46	5	73	0					1,5	
30	1	46	5	73	1	67,7	3	1,97	1,59		
30	1	46	5	73	3	60	2			1,2	
30	1	46	5	73	5	55	2	0,52	2,42	0,9	
30	1	46	5	73	7	71	3	1,68	2,26		
30	1	46	5	73	9	81,3	3	1,89	2,44	1,2	
30	1	46	5	73	11	93	3	1,81	3,22	1,3	
30	1	46	5	73	22	114	3	2,03	4,3		
31	2	63	5	59	0	14	1	0,44	0,88	2,8	
31	2	63	5	59	13	121	3	2,39	5,25	1,5	
31	2	63	5	59	16	159,7	3	5,2	6,67	2,1	
31	2	63	5	59	18	169	3	-		1,7	
31	2	63	5	59	20	96	3	1,94	3,92	1,7	
32	1	73	4	105	0	41	2	0		7,2	78
32	1	73	4	105	1	4,3	1	0			
32	1	73	4	105	3	8	1	0,64	0,83	7,5	
32	1	73	4	105	4	17	1	7,73	2,77		
32	1	73	4	105	5	4,7	1	0,56	0,18	7,6	82
32	1	73	4	105	6	39	1	3,07	1,64	7,2	82
32	1	73	4	105	8	14,7	1	9,53	3,72	7,3	79

32	1	73	4	105	10	3,3	1	0		7,3	81
32	1	73	4	105	12	10,3	1	1,1	0,22	7	81
32	1	73	4	105	21	28,3	1	5,27	2,36		
33	1	79	5	77	0	48,3	2	0		4,9	
33	1	79	5	77	1	36,3	1	2,33	3,05	5,8	76
33	1	79	5	77	2	20	1	0		5,7	75
35	1	76	5	132	0	23	1			2,9	69
35	1	76	5	132	2	9,7	1	0		3,1	84
36	1	81	3	58	0	48	2	3,25	1,62		
36	1	81	3	58	2	39,7	1	1,84	1,58	1	
36	1	81	3	58	4	24	1	5,11	0,69	1,2	
36	1	81	3	58	6	40	2	3,74	1,15	1	
36	1	81	3	58	8	11,3	1	2,9	3,96	1,1	
36	1	81	3	58	24	53,3	2	11,57	1,69	1,2	
37	1	61	6	87	0	46	2	0,48	2,85	1,4	77
37	1	61	6	87	2	42,7	2	2,22	2,7	1,5	76
37	1	61	6	87	14	81	3	2,11	2,18	1	
38	1	79	3	100	0	56,7	2	0		1,4	84
38	1	79	3	100	2	52	2	11,54	4,39	1,6	84
38	1	79	3	100	4	19	1	0,52	3,17	1,8	
38	1	79	3	100	14	23	1	2,07	1,08	1,6	
39	2	69	3	74	0	37,3	1	3,88	2,4	4,6	84
39	2	69	3	74	2	45,3	2	2,22	1,09	4,6	
39	2	69	3	74	4	4,7	1	0		4,3	80
39	2	69	3	74	6	22	1	1,17	1,91		
39	2	69	3	74	8	3,3	1	0,96	0,72	4,8	
39	2	69	3	74	11	10,3	1	0		4,6	
39	2	69	3	74	13						
39	2	69	3	74	24					2,8	84
40	1	47	5	44	0	26,7	1	4,52	1,04		
40	1	47	5	44	2	5	1	0		1,5	
40	1	47	5	44	4	4	1	0		1,5	
40	1	47	5	44	5	5	1			1,8	
40	1	47	5	44	7	36,7	1	-		2,2	
40	1	47	5	44	9	65	3	8,85	5,91	1,5	
40	1	47	5	44	21	76,7	3	3,04	3,92	1,4	
40	1	71	4	42	0	50,3	2	3,34	1,52	0,6	
40	1	71	4	42	2	19	1	0,93	1,55	0,6	
41	1	71	4	42	4	50,3	2	1,85	1,18	1,3	
41	1	71	4	42	6	56,7	2	2,17	0,99	0,8	
41	1	71	4	42	18	30,3	1	0,85	3,67	1	
43	1	66	5	94	0	59	2	0		1,6	
43	1	66	5	94	2	53,5	2			1,1	
43	1	66	5	94	4	54	2	1,31	4,06	1,1	
43	1	66	5	94	6	38,7	1	8,69	3,08	1,5	

43	1	66	5	94	8	52,7	2	0		1,3	
43	1	66	5	94	10	57	2			1,5	
43	1	66	5	94	12	64,3	3			1,6	
43	1	66	5	94	23	62,7	3	20,48	3,64	1,2	
44	1	73	6	91	0					2,4	
44	1	73	6	91	2					2	
44	1	73	6	91	13	39	1	7,11	0,76		
45	1	58	4	71	0	71,3	3	6,98	2,22	1,6	
45	1	58	4	71	2	51,3	2	4,12	1,71	1,9	
45	1	58	4	71	4	60,3	2	3,54	3,98	1,5	
45	1	58	4	71	5	46	2	10,81	3,38	1,3	
45	1	58	4	71	7	76	3	17,33	3,71	1,5	
45	1	58	4	71	9	40	2	9,37	2,82	1,3	
45	1	58	4	71	20	2	1	0		2	
47	2	55	3	42	0	52,7	2	0		0,6	
47	2	55	3	42	2	57,7	2				
47	2	55	3	42	3	65	3	0		0,6	
47	2	55	3	42	5	62	2			0,5	
47	2	55	3	42	7	48	2	0		0,6	
47	2	55	3	42	18	78,7	3	0			
48	2	69	1	78	0	103,3	3	5,33	2,84	1,2	
48	2	69	1	78	5	79,3	3	5,04	2,02	1	
48	2	69	1	78	8	9,3	1	0,34	0,69	1,2	

[1]Gender: 1 = male, 2 = female.

[2]Source of sepsis: 1 = unknown; 2 = cutaneous ; 3 = gastrointestinal ; 4 = urinary; 5 = pulmonary ; 6 = other ;

[3]Time is defined as the number of hours between the dynamic mitoPO$_2$ measurements at time point 'x' and the first dynamic mitoPO$_2$ measurement of each patient.

[4] 1 = Low = mitoPO$_{2_baseline}$ 0-40 mm Hg
2 = Medium = mitoPO$_{2_baseline}$ 41-62.3 mm Hg
3 = High = mitoPO$_{2_baseline}$ >62.3 mm Hg

[5] MitoVO$_{2_max}$ = 0 (Dynamic mitoPO$_2$ measurement without inducible mitoVO$_2$)

[6] Insufficient fit performance

APACHE IV score = Acute Physiologic and Chronic Health Evaluation IV score; mitoPO$_{2_baseline}$ = baseline mitochondrial oxygen tension; mitoVO$_{2_max}$ = maximum oxygen consumption; RMSE = root mean squared error; ScvO$_2$ = central venous oxygen saturation